



Adhesively Bonded Steel Structures

by

Man-Shin Tan
Nozhan Sharifian

Diploma work No. 52/2011

at Department of Materials and Manufacturing Technology
CHALMERS UNIVERSITY OF TECHNOLOGY
Göteborg, Sweden

Diploma work in the Master program Advanced Engineering Materials

Performed at: Volvo Car Corporation
405 31 Göteborg, Sweden

Supervisor(s): Johnny K Larsson
Volvo Car Corporation
Department 93620, PVÖS22
SE-405 31 Göteborg, Sweden

Examiner: Prof. Maria Knutson Wedel
Department of Materials and Manufacturing Technology
Chalmers University of Technology, SE-412 96 Göteborg

Adhesively Bonded Steel Structures

Man-Shin Tan
Nozhan Sharifian

© Man-Shin Tan, Nozhan Sharifian 2011.

Diploma work no 52/2011
Department of Materials and Manufacturing Technology
Chalmers University of Technology
SE-412 96 Göteborg
Sweden
Telephone + 46 (0)31-772 1000

[CHALMERS Reproservice]
Göteborg, Sweden 2011

Adhesively Bonded Steel Structures
Man-Shin Tan
Nozhan Sharifian
Department of Materials and Manufacturing Technology
Chalmers University of Technology

SUMMARY

The amount of weld bonding on thin sheet steel structures has increased dramatically since year 2000. Weld bonding is used for improvement of stiffness, durability, strength, crash performance and weight reduction of car body structures. This thesis work focus on the effect of adhesive in crash performance for High Strength Steel (HSS) and Ultra High Strength Steel (UHSS).

The influence of epoxy-based and rubber-based adhesives was investigated in hat-lid beams. The beams were tested in different sheet thicknesses (1,5 mm or 1,0 mm), spot weld spacing (80 mm or 40 mm), steel grades (Usibor or DP600) and joining methods (spot welding or weld bonding). In the case of weld bonded beams, the joints were bonded with either epoxy- based or rubber-based adhesive. The beams without adhesive were used as reference.

The beams were tested in 4-point bending in computer simulations and in experimental tests. The weld bonded beams were compared with the resistance spot welded beams, in order to distinguish which combination was able to reduce the deformation. The possibility to increase spot weld spacing of weld bonded beams for different thicknesses was also studied.

The simulations results were validated by experimental tests of 4-point bending. Rubber-based and epoxy-based adhesives had positive influence in deformation reduction and flange separation in DP600. The contribution of adhesive was small in Usibor.

Keywords: adhesive, weld bonding, high strength steel, deformation reduction

Acknowledgments

This thesis work is the final step of our master studies of Advanced Engineering Materials at Chalmers University of Technology (CTH), Gothenburg, Sweden. The work has been carried out at Volvo Car Corporation (VCC) (Department 93620) in Gothenburg between December 2010 and May 2011.

We would like to thank our supervisor Johnny K Larsson, VCC, for his tremendous support and guidance, and also our supervisor and examiner Prof. Maria Knutson Wedel, CTH, for her kind advice.

Special thanks to people in the Body Engineering Department Camilla Wästlund, Henrik Ebbinger, Mikael Fermer and Richard Johansson for their help and friendliness during our thesis work at Volvo Car Corporation.

We also want to thank all people who helped us during our thesis study, Ola Wiberg, Gert Larsson, Joel Lundgren, Benny Andersson for making it possible to complete this work.

Gothenburg, May 2011

Man-Shin Tan and Nozhan Sharifian

List of words and abbreviations

AHSS	Advanced High Strength Steel
ANSA	Advanced CAE pre-processing tool
B-pillar	Vertical roof support and load-carrying component in the car
CAE	Computer Aided Engineering
DP	Dual-Phase steel
FE	Finite element
HAZ	Heat affected zone
HSS	High strength steel
LS-DYNA	Finite element software
MS	Mild Steel
UHSS	Ultra high strength steel
Usibor	Boron steel coated with Aluminum-Silicon [Al-Si]
VCC	Volvo Car Corporation
VHSS	Very High Strength Steel

Table of content

1. INTRODUCTION.....	1
1.1 BACKGROUND	1
1.2 OBJECTIVE.....	1
1.3 METHOD.....	2
1.4 CONSTRAINTS.....	2
1.5 HYPOTHESIS	2
2. THEORY	5
2.1 STEEL GRADES USED IN THE AUTOMOTIVE INDUSTRY	5
2.2 ADHESIVE BONDING AND WELD BONDING	5
2.2.1 Advantages of weld bonding.....	6
2.2.2 Concerns about epoxy-based adhesives	6
2.3 SPOT WELDING	6
2.4 DUAL PHASE STEEL.....	8
2.4.1 Heat treatments of dual phase steels	8
2.4.2 The role of alloying elements.....	9
2.5 BORON STEEL	9
2.5.1 Heat treatments of the boron steels.....	9
2.5.2 The role of alloying elements.....	11
2.6. 4-POINT BENDING.....	11
3. METHOD	13
3.1 GENERAL.....	13
3.1.1 Geometry of the beams and test setup	13
3.1.2 Weld nugget size.....	14
3.2 COMPUTER AIDED ENGINEERING (CAE)	15
3.2.1 Searching for a suitable adhesive model in CAE	15
3.2.2 Searching for desirable deformation in CAE	16
3.2.3 Planning the test matrix.....	16
3.3 MANUFACTURING OF BEAMS	17
3.4. 4-POINT BENDING IN EXPERIMENTAL TESTS	19
3.4.1 Measurements of deformation	20
4. RESULTS	21
4.1 CAE RESULTS OF DP600 AND USIBOR.....	21
4.1.1 Finding adhesive model in CAE.....	21
4.1.2 Finding desirable deformations in CAE.....	22
4.1.3 Results of 4-point bending of DP600 in CAE.....	22
4.1.4 Appearance of flanges DP600 beams.....	23
4.1.5 Results of 4-point bending of Usibor in CAE	25
4.1.6 Appearance of flanges in Usibor beams.....	25
4.1.7 Results of spring back.....	26
4.1.8 Summary of CAE simulations.....	27
4.2 EXPERIMENTAL TEST RESULTS OF DP600.....	27
4.2.1 Comparing thickness and bonding of DP600.....	27
4.2.2 Comparing the behavior of adhesive in DP600	29
4.2.3 Appearance of flanges and spot welds in DP600 beams	30
4.3 EXPERIMENTAL TEST RESULTS OF USIBOR.....	35
4.3.1 Comparing thickness and bonding of Usibor	35
4.3.2 Comparing the behavior of adhesive in Usibor.....	36

4.3.3 Appearance of flanges and spot weld in Usibor beams.....	38
4.4 SCATTER OF DEFORMATION.....	40
4.5 SUMMARY OF THE EXPERIMENTAL TESTS (STATIC DEFORMATION).....	41
4.6 DYNAMIC DEFORMATION.....	42
4.6.1 Comparing dynamic deformation with static deformation.....	43
4.7 CORRELATION BETWEEN CAE SIMULATIONS AND EXPERIMENTAL TESTS	43
5. DISCUSSION	45
6. CONCLUSIONS	47
7. FUTURE WORK AND RECOMMENDATIONS	49
REFERENCES.....	51
APPENDIX 1.....	55
APPENDIX 2.....	56
APPENDIX 3.....	57
APPENDIX 4.....	58
APPENDIX 5.....	59
APPENDIX 6.....	65
APPENDIX 7.....	70
APPENDIX 8.....	71

1. Introduction

1.1 Background

One of today's most important issues in the automotive industry is to reduce the weight of the vehicle. The main purpose of reducing the weight is to reduce fuel consumption and consequently diminish the CO₂ emissions. Studies show that by reducing 100 kg weight, the CO₂ emission will be reduced with 3 to 5 percent depending on vehicle size and powertrain solutions [1]. 20% of the total vehicle weight corresponds to the car body. Therefore, it is beneficial to reduce the weight of the car body. One of the significant ways of reducing the body weight is to use High Strength Steel (HSS). These steels make it possible to reduce the thickness of the component and at the same time provide high strength. Nowadays HSS has been frequently used in car body constructions. The safety cells of today's cars mainly consist of Very High Strength Steel (VHSS) and Ultra High Strength Steel (UHSS).

Weld bonding is a hybrid process which is a combination of resistance spot welding and adhesive bonding. This method is commonly used in the automotive industry. The purpose of the spot welds is to fix the body component in alignment until the adhesive becomes fully cured. Spot welds usually impose large stress concentration in the heat affected zone (HAZ) in boron steel.

Epoxy-based structural adhesives are commonly used in car body structures, but most of these adhesives are hazardous and require special handling¹. Safety equipment is required for handling the adhesive and protective working clothes need to be washed separately. The problem with today's rubber-based adhesives is that although they are less hazardous, they have lower strength and lower fatigue performance than the epoxy-based adhesives.

1.2 Objective

The purpose of the thesis work was to investigate the deformation of beams which has been tested in 4-point bending. The purpose was to:

- Investigate the contribution of adhesive.
- Investigate if adhesive reduces deformation.
- Investigate whether adhesive prevents spot failure.
- Investigate whether the sheet thickness and spot weld spacing affect the deformation.

The 4-point bending test was also simulated in a computer program in order to:

- Compare the Finite Element model (FE-model) of adhesive with experimental tests and investigate the reliability of the adhesive model-card.

¹ In Sweden this is regulated by the Thermoset Plastics legislation. VCC has interpreted the legislation as amongst other things, for example the working clothes.

The beams were made of either boron steel (Usibor) or dual-phase steel (DP600) with different sheet thicknesses and spot weld spacing.

1.3 Method

The beam models (FE-models) were built in the ANSA program and the 4-point bending simulations were made in LS-DYNA. All the tests were simulated before the experimental tests, in order to find the correct velocity and masses for the experimental tests. In the simulation program, various loading cases, different sheet thicknesses, different spot weld spacing and joining combinations were tested. The experimental tests were carried out on 70 beams and the results were analyzed. The correlation between results from Computer Aided Engineering, (CAE) and experimental tests were also examined. In the end of the project new knowledge about the adhesives and steel grades were obtained (see figure 1.1).

1.4 Constraints

In this project, the tests were limited to only 4-point bending tests and the beams had one specific geometry. There was an interest of performing axial crush tests to evaluate weld bonded DP600 beams, but it was excluded from the scope of this thesis work due to time limitations. Furthermore it was planned to test the beams in three thicknesses (1,0 mm, 1,2 mm and 1,5 mm), but it was necessary to reduce the number of tests. The 1,2 mm sheet thickness beams were removed from the test plan.

1.5 Hypothesis

The following hypotheses are based on the literature survey; old test report and scientific articles about 4-point bending and spot welding. It was possible to state these hypotheses with the knowledge about the materials and joining methods.

Spot welded structure

- If the material fails or cracks, the crack initiation and propagation will start around the spot weld.
- Long weld time and high current will be necessary to spot weld thick sheet beams.

Weld bonded structure

- Weld bonded structures will have uniform stress distribution around the spot welds, due to the use of adhesive. It will also have the ability to withstand higher forces with less deformation.
- When the spot weld spacing is long, the adhesive will carry the load. Long spot weld spacing is tough for the adhesive and it will cause failure of the adhesive.

In general, the deformation of the beams should be dependent upon the sheet thickness. Thick sheets should be able to withstand higher force and energy than thin sheet beams. Moreover, beams with large spot weld spacing should have larger deformation than the beams with short spot weld spacing, because large distances are tough for the joint.

Flow chart of the working procedure

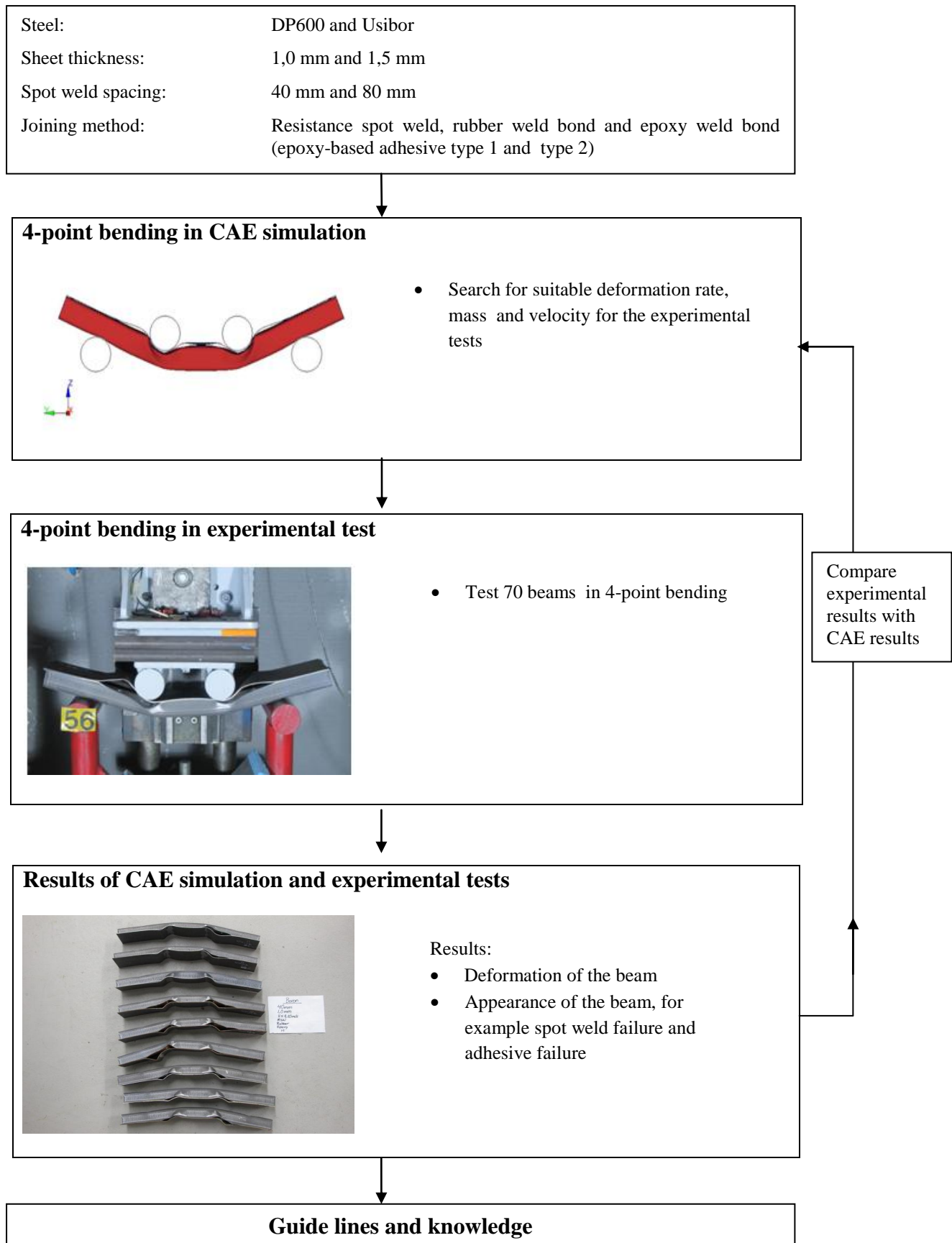


Figure 1.1. Flow chart of the working procedure.

2. Theory

2.1 Steel grades used in the automotive industry

The use of High Strength Steel (HSS) and Ultra High Strength Steels (UHSS) as a replacement of mild steel (MS) has increased significantly since year 2005. Today it is possible to obtain the same performance with thinner HSS than corresponding Mild Steel and consequently reduce the weight [1]. These properties are desirable in the car body and safety cabin.

B-pillar is a part of car body which is made of high strength steels. B-pillars are vertical roof supports which carry the load from the front to the rear side doors. Besides this, it has the task to take the force in the event of a side crash. B-pillars are typically thin walled and spot welded. With the use of HSS it is possible to make B-pillars considerably thinner and lighter than corresponding B-pillars made of MS [2]. HSS also contributes with better vehicle safety due to the high strength [3].

A car body consist of different metals, such as Ultra High Strength Steel (UHSS), Extra High Strength Steels (EHSS), Very High Strength Steels (VHSS), High Strength Steels (HSS), Mild Steels (MS) and Aluminum (AL) (see appendix 1). Figure 2.1 illustrates the different steels in a car body and shows the position of the B-pillar in a car. In the predecessor V70 model, 58 % of the car was made of mild steels, but in the new V70 model only 30% was made of mild steel. The use of UHSS (such as boron steel) has increased to 10 % in the new model.

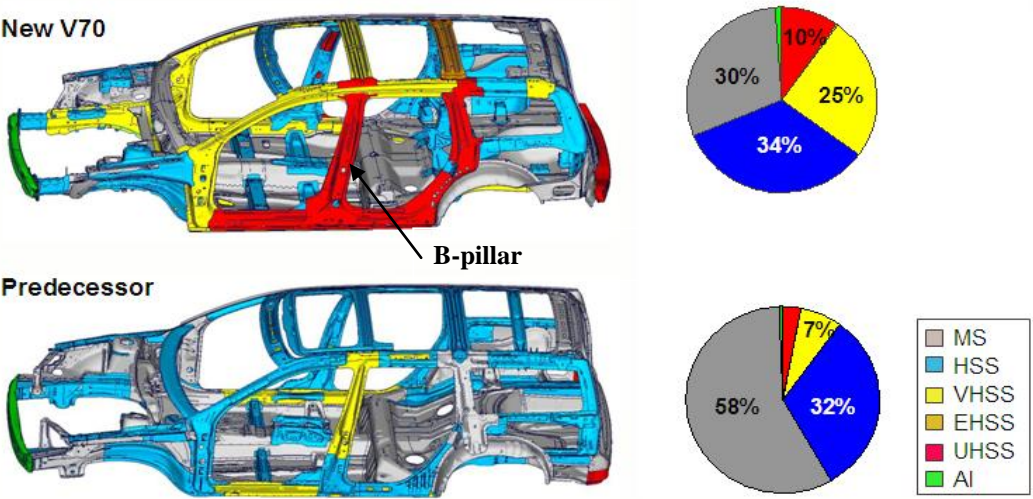


Figure 2.1 Comparing a predecessor model of Volvo with a new model. The use of VHSS and UHSS has increased in the car body structure[4].

2.2 Adhesive bonding and weld bonding

In the automotive industry, weight has an important effect on the fuel consumption. There is a tendency to use thin-wall structures in order to diminish weight and fuel consumption. The car body is approximately one fifth of the total vehicle weight. One way to reduce weight is to

down-gauge the steel structure. It is possible to fasten these structures by using adhesive (typically an epoxy-based paste or rubber-based adhesive) in combination with spot welds. This method is called weld bonding. The adhesive is cured in an oven with adequate temperature and time.

2.2.1 Advantages of weld bonding

Weld bonding increases the stiffness and enables better crashworthiness of car body structures. It also affects the fatigue performance and Noise, Vibration and Harshness (NVH). Studies confirm that, adhesives reduce the peak stress in the spot welds and offer an even stress distribution [5]. The weld bonded structures have higher energy absorption and smoother energy distribution in the joint than resistance spot welded structures [6][7]. In addition, weld bonding results in a cost reduction of the whole vehicle design by reducing the number of spot welds[8].

Epoxy-based adhesives are thermosetting adhesives which exhibit high tensile strength in both dynamic and static loading conditions. They also have good fatigue resistance. In general, rubber-based adhesives exhibit lower tensile and shear strength than epoxy-based adhesives, besides they have high cleavage strength [9].

2.2.2 Concerns about epoxy-based adhesives

The use of weld bonded structures in the automotive industry is increasing constantly. Adhesives result in better performance in many aspects, but many of them can be hazardous to humans. The working atmosphere needs to be constantly evacuated from fumes of epoxy containing polyurethane. In order to reduce the risk of harming operators, companies invest a considerable amount of money on robotic applications and powerful ventilations [10]. Epoxy-based adhesives may cause skin redness, allergic respiratory reaction and eye irritation. Fumes of polyurethane could be the main source of occupational asthma for the operators who are exposed to it [11]. Excess adhesive should be wiped off from the components in order to prevent spreading to other places.

Due to the increasing consumption of adhesives and the environmental hazardous effect of epoxy-based adhesives, companies use other adhesives (for example rubber-based adhesives). The rubber-based adhesives should contain environmental friendly characteristics and need to fulfill requirements of strength, fatigue and stiffness.

2.3 Spot welding

Spot welding is widely used in the automotive industry due to the short process time, small heat affected zone, low cost and good weld quality. Resistance spot welding (RSW) is a process where two or more contacting metals are joined together without filler material. An appropriate pressure is required over a short period of time in order to keep molten material in the weld zone. The required pressure is applied by hydraulic, pneumatic or electric systems. Spot welding makes it possible to deliver a large amount of heat into a spot at a very short time and creates a small Heat Affected Zone (HAZ) [12].

The amount of energy and heat, which is produced during the spot welding operation, is expressed by: (see equation 1.1) [13]

$$E = RI^2t \quad (1.1)$$

E = heat energy [J]

I = current [A]

R = electrical resistance [Ω]

t = time that the current is applied [s]

Resistance spot welding is usually used for sheet metals and it requires a double-sided access (see figure 2.2). Thick sheets are usually difficult to weld, because the heat will spread over a large area around the spot and require longer welding time and higher current. The heat affected zone (HAZ) is larger for thick sheets and it is difficult to spot weld three sheets especially when the outer sheet is thinner than the inner sheets. It is almost impossible to get the same amount of heat for all sheets [12][13].

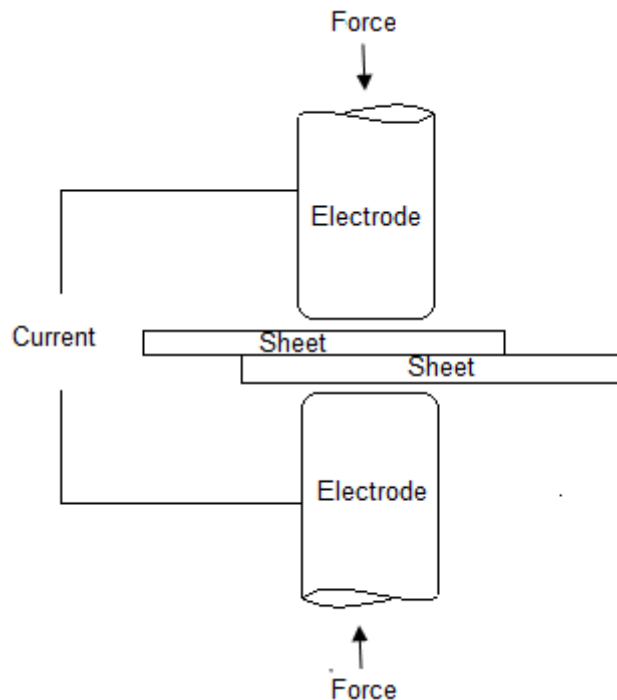


Figure 2.2: Resistance spot welding (the welding method needs double-sided access)

In order to get a proper weld, it is important to have correct relation between electrode force, diameter of the electrode contact surface, squeeze time, welding time, hold time and welding current.

2.3.1 Spot welding of different steels

Compare to mild steel, boron steel needs to be welded with shorter welding time and higher welding current [13]. Therefore more powerful welding guns are required for welding boron steel. Same as boron steels, dual phase steels (DP) need high welding current, in order to reduce welding time and burn mark size [14]. During the welding process of DP martensite

will form. The martensite will increase the risk of interfacial fracture in the weld nugget. One method of reducing the risk of having fracture is to reduce the hardness by pre-and post heat treatment of the steel [15]. High strength steels exhibit high fatigue life in low loading cycles [16]. In general, welds are the initiation site of fatigue failure.

2.3.2 Failure in spot welds

Plug failure occurs when the weld nugget is completely pulled out from the sheet. Spot welds can also fail by partial plug failure, which means that the whole plug is not pulled out. Interfacial fracture and partial plug fracture are two types of defects that might occur in boron steel (see figure 2.3) [17].

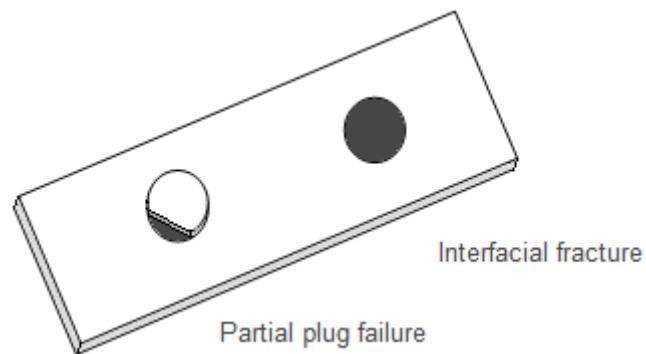


Figure 2.3: Partial plug fracture and Interfacial fracture

2.4 Dual phase steel

Dual phase steel has good formability together with good mechanical properties, which is one of the main drivers of using them. Dual phase steel is categorized among the Very High Strength Steels (VHSS) [18]. They have good initial work hardening, high energy absorption and it is possible to reduce the weight by using thinner gauges of sheet material. Dual phase steel is frequently used in the automotive industry for body panels, bumpers and hoods. Nowadays, dual phase steel is used as a replacement of mild steel in the automotive industry.

Dual phase steel consists of a soft matrix of ferrite and hard islands of martensite [19]. The strength will generally increase with increasing volume fraction of martensite. Due to the existence of a continuous ferritic matrix, DP steels exhibit excellent ductility. During deformation the strain concentrates in between the soft ferritic grains. The ferritic phase is surrounded by islands of martensite and results in a very high work hardening ability [19].

2.4.1 Heat treatments of dual phase steels

The dual phase steel sheets are usually delivered to the production line in cold rolled or hot rolled condition from the supplier. The steel sheets are heat treated before delivery. During the heat treatment the temperature is raised to the two phase region (ferrite and austenite region) and kept for some time. Annealing is performed to stabilize the amount of austenite to obtain the martensitic-ferritic microstructure after quenching [20]. The specific time and temperature depends on the desired properties of the steel. By having higher amount of retained austenite, the ductility of the steel will increase. The steel is quenched from the two phase region and austenite alters to martensite. Dual phase steel has yield strength of 340 MPa

and an ultimate tensile strength of 600 MPa after quenching [21]. The strength can be further increased by work hardening and bake hardening [22].

2.4.2 The role of alloying elements

The main alloying elements in DP steels are carbon (C), silicon (Si) and manganese (Mn). Manganese is an austenite forming element which increases the hardenability of the steel. The silicon in dual phase steel increases the tensile and yield strength [19]. Other elements that are present in DP steel are chromium (Cr), molybdenum (Mb), vanadium (V) and nickel (Ni). They increase the hardenability of the steel. Carbon causes formation of martensite during the quenching of the steel, therefore the hardness of steel will increase [19].

The strength of the martensite is mainly due to the C content and the annealing process. The strength of the ferrite comes from the grain boundaries [22]. During annealing at 750-850 °C the austenite starts to nucleate from the grain boundaries. The austenite grains grow until all the pearlite or cementite is dissolved [22]. Table 2.1 shows the common alloying elements in DP600 and DP800 steel.

Table 2.1 Alloying elements in DP600 and DP800 [%][23]

Grade	C	Mn	Si	S	P	Al	N₂
DP600	0,100	1,100	0,300	0,008	0,060	0,02-0,06	0,009
DP800	0,110	1,120	0,330	0,009	0,070	0,02-0,06	0,009

2.5 Boron steel

Boron steel is an Ultra High Strength Steel which is used in the automotive industry due to its superior properties. It is as mentioned in chapter 2.1 that boron steel is used in safety components such as B-pillars (due to the high strength). Hot formed boron steel has a limited elongation, but it has high strength. Boron steel has yield strength of 1000 MPa and an ultimate tensile strength of 1500 MPa, which is almost three times higher than regular high strength steel.

2.5.1 Heat treatments of the boron steels

There are two ways of hot forming boron steel. It is possible to form it directly or indirectly. The strength of boron steel increases by heating, stamping, pressing and cooling operations. Before the hot forming operation, the steel has relatively low strength. The ultimate tensile strength is approximately 600 MPa and the constituents in the initial microstructure of boron steel are ferrite, pearlite and carbide [24]. Figure 2.4 shows the strength of the steel before and after the hot forming process.

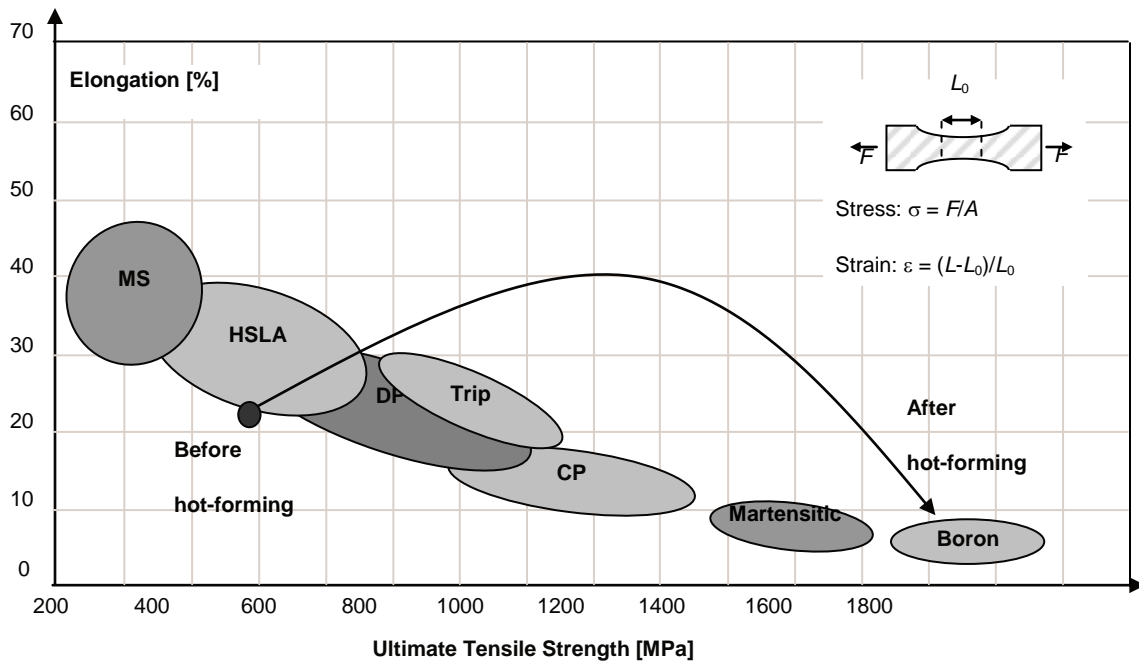


Figure 2.4: Different common steels which are used in the automotive industry, high strength boron steel before and after hot forming [25].

In the direct forming process, stamping, forming and hardening are done in one operation. Figure 2.5 shows the procedure of hot stamping. The sheets are heated to 900-950 °C for 4-10 minutes, with the purpose of obtaining homogeneous austenite microstructure in the material [26]. After the heat treatment, the sheets are sent from the furnace to the hot forming tool. The temperature is lowered from the austenitization temperature to 650-850 °C. At this temperature the material is easy to form and the sheets are stamped and formed into the desired geometry. After that, the sheets are cooled in a die. The time and pressure, required for the cooling depends on the sheet thickness. During cooling, austenite transforms into martensite and the final constituent of boron steel is lath martensite.

In the indirect method the sheets are cold formed into nearly final product shape in a conventional die before the heating, stamping, pressing and cooling operations. The pre-forming is the main difference between direct and indirect forming. (Direct forming does not have this additional pre-forming step.) The advantage of indirect forming is that the pre-forming enables the final product to have complex shapes. Meanwhile it is difficult to create complex shapes in direct forming. The procedure of indirect forming are similar to direct forming. It means that the sheets are austenitized after the cold drawing operation followed by stamping and cooling in a die. Figure 2.6 shows the indirect forming method.

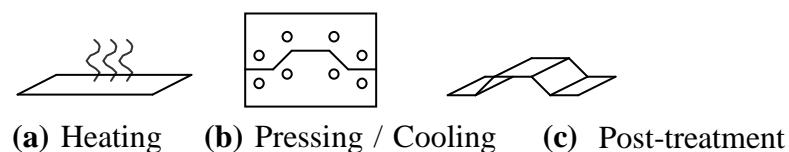


Figure 2.5: The procedure of direct forming [27].

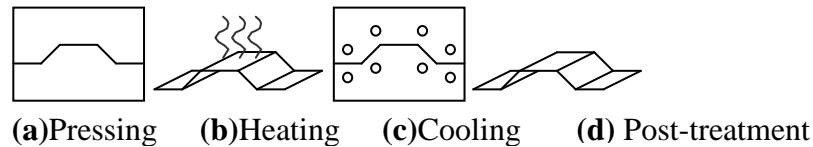


Figure 2.6: The procedure of indirect forming[27].

2.5.2 The role of alloying elements

The alloying elements contribute to the hardness and strength of the steel. Carbon (C), silicon (Si), manganese (Mn), phosphor (P), sulfur (S) and chromium (Cr) are the alloying elements of boron steel. Table 2.2 shows the chemical composition of alloying elements for boron steel.

Table 2.2: The chemical composition of boron steel [%][27]

Element	C	Si	Mn	P	S	Cr	B
Min	0,200	0,200	1,000	-	-	0,150	0.0015
Max	0,250	0,350	1,300	0,025	0,015	0,250	0.0050

The carbon content in boron steel is 0.20-0.25%. Carbon increases the strength and hardness, but the carbon content should not exceed 0.8%. If it exceeds 0.8%, the carbon will lose its hardening effect. Boron is added in the steel to increase the hardness (0.001-0.004 % boron) [28]. Boron as an alloying element increases the hardening ability by moving the transformation curves to the right in a Time-Temperature-Transformation-diagram, (TTT-diagram) it delays the formation of pearlite, ferrite and bainite [24].

2.5.3 Specifically about Usibor

Usibor is a special type of boron steel and it is especially developed for automotive use. Usibor has an Al-Si-coating which is 20-33 μ m thick, protecting the steel against oxidation and decarburizing [29]. The plating layer of Al-Si has a melting point of approximately 600°C [30]. During the heat treatment the Al-Si-coating transforms into an Al-Si-Fe coating. The Fe diffuses into the Al-Si layer and the coating becomes 35 μ m thick and adheres to the steel [31].

2.6. 4-point bending

The main purpose of the 4-point bending test is to determine the strength of test specimens. In 4-point bending tests, the load is applied at two points of the beam. The load falls with a certain velocity on the beam and creates a deformation. Another possibility of using 4-point bending is to test the performance of joints for assembled B-pillars. In order to simplify the test specimen, it is possible to deform the beams in 4-point bending. Figure 2.7 shows a simplified beam model, which is tested in 4-point bending.

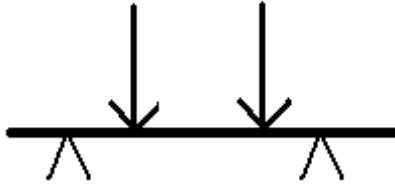


Figure 2.7: 4-point bending test

Defects such as inclusions and pores create local stress in the material and are often the initial crack points. Therefore, the test results vary from each test specimen depending on the number of defects. If the beam is welded it usually starts to crack from the weld. The weld is the initial site of crack, because it may have defects such as pores and inclusions, which is lowering the material strength.

3. Method

This part is describing the geometry of the beams, welding and testing of the beams. It also describes the computer program.

3.1 General

Table 3.1 shows the different steel grades, spot weld spacing, sheet thickness and the joining methods of the beams.

Table 3.1: Parameters of the beams

Steel	DP600 and Usibor
Spot weld spacing	40 mm and 80 mm
Sheet thickness	1,0 mm and 1,5 mm
Joining method in the CAE simulations	Resistance spot weld Epoxy weld bond (epoxy-based adhesive type 1, the regular one)
Joining method in the experimental tests	Resistance spot weld Epoxy weld bond (epoxy-based adhesive type 2, especially developed for press hardened steel) Rubber weld bond

3.1.1 Geometry of the beams and test setup

DP600 and Usibor steel beams were manufactured with either 40 mm or 80 mm spacing between the spot welds. The center spot (the spot positioned 250 mm from the end) was kept in both 40 mm and 80 mm spot weld spacing. The position of the impactor was selected to not hit on the spot welds directly.

The impactor was made of thick and rigid steel, which could withstand high amount of energy without deformation. (The role of the impactor was to hit and create a deformation of the beam.) Figure 3.1- 3.3 shows the geometry of the beams. Figure 3.4 shows the geometry of the impactor. The lid was facing upwards in the fixture, which means the impactor hit the lid first.

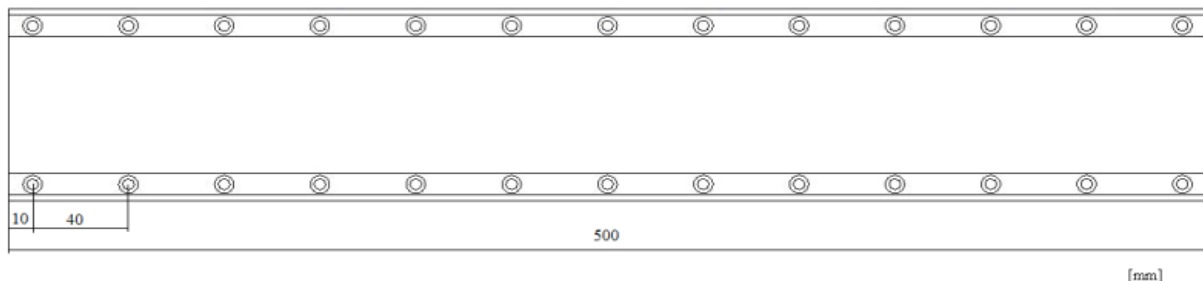


Figure 3.1: A weld bonded beam with 40 mm distance between the spot welds. The adhesive line is visible in this beam.

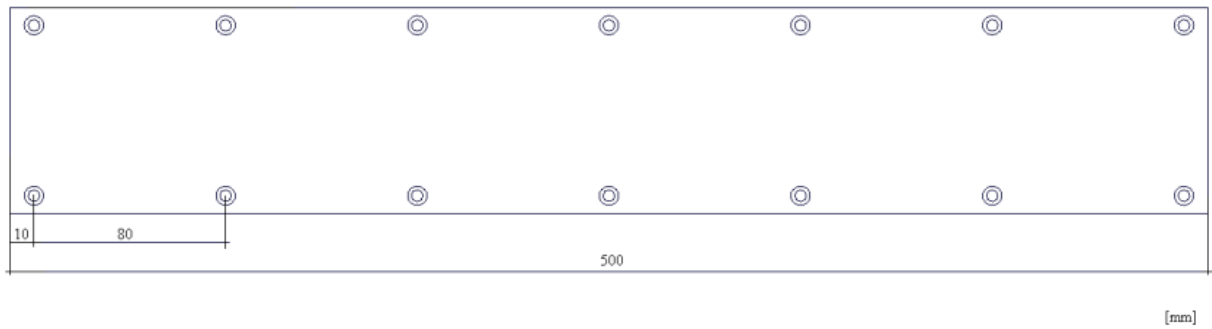


Figure 3.2 A resistance spot welded beam with 80 mm distance between the spot welds. The adhesive line is not visible in this beam.

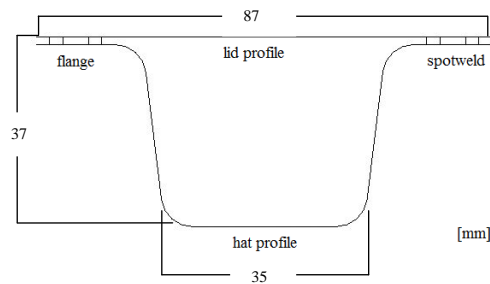


Figure 3.3 Cross section of a beam. The flat part is called lid and the U-shaped profile is called hat.

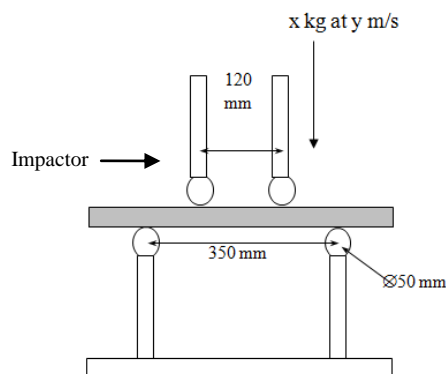


Figure 3.4 The geometry of the impactor. The two circles on top are the cross section of the impactor. The two circles below are showing the fixture in which the beams lie.

3.1.2 Weld nugget size

The beams were manufactured with two different sheet thicknesses 1,0 mm and 1,5 mm and the weld nugget was selected as two different sizes. Table 3.2 shows the nugget size for each sheet thickness.

Table 3.2 The nugget diameter size for different thicknesses.

Thickness [mm]	1,0	1,5
Nugget diameter [mm]	4,0	4,9

The weld nugget diameter was calculated by American Welding Society (AWS) standard, (see equation 3.1).

$$d = 4\sqrt{t} \quad (3.1)$$

d = weld nugget diameter [mm]

t = sheet thickness [mm]

3.2 Computer Aided Engineering (CAE)

There were two main purposes of conducting CAE simulations. The first reason was to search for a proper test setup for the experimental tests. The second reason was to compare the results from the simulation tests with the experimental tests and verify the accuracy of the material card for the adhesive in ANSA.

ANSA is an advanced Computer Aided Engineering (CAE) pre-processor for finite element (FE) analysis and it was used to model the hat-lid beams. The FE-solver LS-DYNA calculated the deformation of the beams. The different beam versions were created by changing sheet thickness, spot weld spacing, steel grade and type of adhesive in the computer model. Different amount of deformation of the beam was created by changing the velocity and mass of the impactor. The results were analyzed with Animator software. Animator showed the animation of the 4-point bending tests. In the program it was possible to measure the deformation of the beams during impact (dynamic deformation). Figure 3.5 shows the beam and impactor in the simulation program.

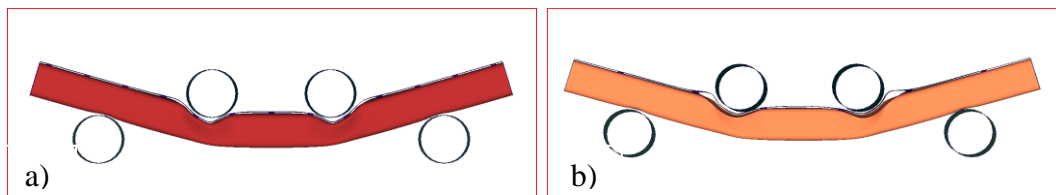


Figure 3.5: Simulation of beams after a hit with the impactor on top. Picture a) shows 40 mm spot weld spacing and picture b) shows 80 mm spot weld spacing.

3.2.1 Searching for a suitable adhesive model in CAE

In order to find the correct adhesive model, four different material cards were evaluated. (A material card is a material model, which is created by dynamic and static tests on materials.) The material cards for the rubber-based adhesive and epoxy-based adhesive (type 1, the regular one) were investigated. The evaluations of epoxy-based adhesive were done on three different tuned models.

3.2.2 Searching for desirable deformation in CAE

The approach of the simulations were to have two levels of deformation of the beams. By having two levels of deformation it was possible to compare the thicknesses and spot weld spacing of the beams at the same deformation. The “high” and “low” deformation was chosen with the following considerations:

- The beams should deform adequately
- Material failure should be avoided (risk with Usibor)

The beams with 40 mm spot weld spacing and without adhesive was used as the reference. The deformation levels were achieved by changing the mass of the impactor. In the simulation program, the velocity was kept constant at 10.0 m/s for all tests (see appendix 2 for the masses).

3.2.3 Planning the test matrix

The 1,2 mm thickness was deleted from the test matrix, since it was more desirable to test the extremes of the thicknesses. The spacing between spot welds were 40 mm and 80 mm. Table 3.3 shows the motivations of choosing the specific test setup. Table 3.4 shows the planned test matrix.

Table 3.3: Motivations of choosing a specific test setup.

Dual phase beams (DP600)	Boron beams (Usibor)
<ul style="list-style-type: none"> • DP600 was tested in two thicknesses (1,0 mm and 1,5 mm) and two spot weld spacing (40 mm and 80 mm) and in three joining methods (resistance spot weld, rubber weld bond and epoxy weld bond (adhesive type 2)). • The epoxy based adhesive (type 2) was developed especially developed for press-hardened steels. Therefore, DP-beams with 1,0 mm thickness and 80 mm spot weld spacing were not tested with epoxy based adhesive. 	<ul style="list-style-type: none"> • Usibor was tested in two thicknesses (1,0 mm and 1,5 mm) and in one spot weld spacing (40 mm) and in two joining methods (resistance spot weld and epoxy weld bond (adhesive type 2)). • The rubber weld bonded beams were tested in thickness 1,0 mm only, since rubber-based adhesive showed low contribution of adhesive (at 1,5 mm beams) in the CAE simulations. • The Usibor beams were only limited to 40 mm spot weld spacing, because 80 mm spot weld spacing had more effect on dual phase beams (based on CAE results).

The tests were carried out in 2-3 repetitions. The 1,5 mm DP600 beams were only tested in two repetitions, due to lack of steel sheets. In order to reduce the number of tests further, all the beams with 80 mm spot weld spacing were performed in only two repetitions. The total number of tests was 70 and a few extra beams were manufactured to calibrate the drop tower device (see appendix 3). (When the calibration beams had the correct settings and deformations, they were included into the test matrix.)

Table 3.4 The planned test matrix.

Version	Material	Thickness [mm]	Joining method	Spacing [mm]	Deformation [high or low]
1	DP	1,0	RSW	40	H
2	DP	1,0	Rubber+RSW	40	H
3	DP	1,0	RSW	40	L
4	DP	1,0	Rubber+RSW	40	L
5	DP	1,0	RSW	80	H
6	DP	1,0	Rubber+RSW	80	H
7	DP	1,0	RSW	80	L
8	DP	1,0	Rubber+RSW	80	L
9	DP	1,5	RSW	40	H
10	DP	1,5	Rubber+RSW	40	H
11	DP	1,5	Epoxy+RSW	40	H
12	DP	1,5	RSW	40	L
13	DP	1,5	Rubber+RSW	40	L
14	DP	1,5	Epoxy+RSW	40	L
15	DP	1,5	RSW	80	H
16	DP	1,5	Rubber+RSW	80	H
17	DP	1,5	RSW	80	L
18	DP	1,5	Rubber+RSW	80	L
19	Boron	1,0	RSW	40	H
20	Boron	1,0	Rubber+RSW	40	H
21	Boron	1,0	Epoxy+RSW	40	H
22	Boron	1,0	RSW	40	L
23	Boron	1,0	Rubber+RSW	40	L
24	Boron	1,0	Epoxy+RSW	40	L
25	Boron	1,5	RSW	40	H
26	Boron	1,5	Epoxy+RSW	40	H
27	Boron	1,5	RSW	40	L
28	Boron	1,5	Epoxy+RSW	40	L

3.3 Manufacturing of beams

The Usibor profiles were delivered in hot-formed condition, which means that the hat and lid profiles were ready to be joined in the condition they arrived. The DP600 profiles were delivered as rolled sheets, which meant that they needed to be shaped into hat-profiles. Therefore, the bending process and the final cutting were done at Volvo.

The DP600 sheets had delivery oil layer on the surface. In order to make sure that all the DP600 beams had an oil layer compatible with the adhesive on flange surface, they were degreased with a solvent (n-Heptane) and brushed on with a known oil (Aral Ropa 4093) (see figure 3.6).

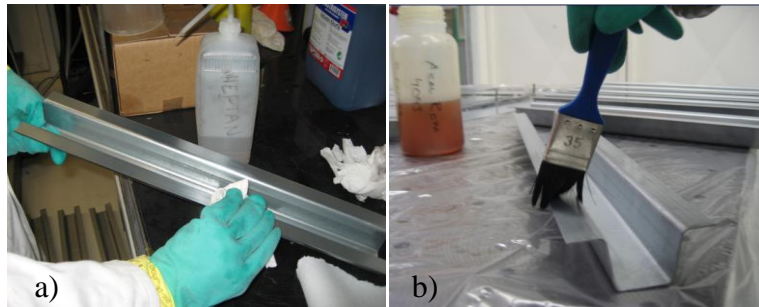


Figure 3.6: a) Degreasing with n-Heptane and b) brushing on Aral Ropa 4093

The adhesive was manually applied with an adhesive gun at approximately 55 °C and at a pressure of 5 Bar. The heat made the adhesive viscous and easier to apply. The aim was to fill the whole flange with adhesive. The lid was attached to the hat-profile. The attachment was done immediately in order to prevent moisture absorption. Figure 3.7 shows the procedure of applying adhesive. The same procedure was used to apply adhesive on Usibor, apart from the degreasing procedure.

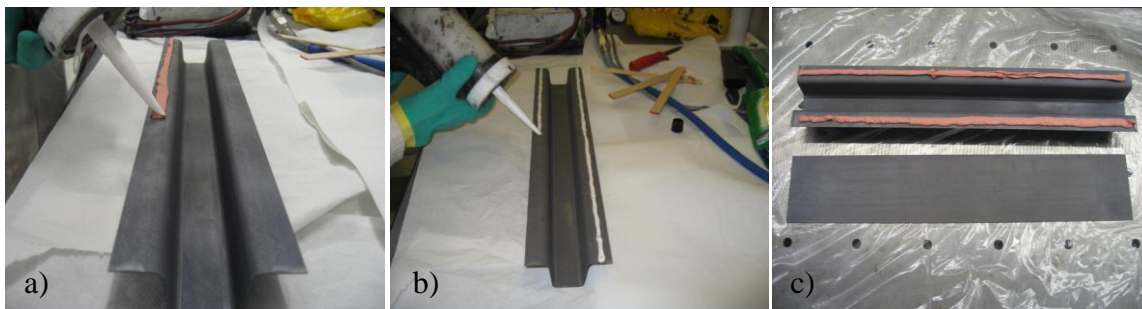


Figure 3.7: a) Applying rubber based adhesive b) Applying epoxy based adhesive (type 2) c) Hat and lid before assembly

3.3.1 Spot welding

The spot welds were made by a robot gun (Bosch 6000, KRC1). It was desirable that 1,0 mm thick sheets had a nugget diameter of 4,0 mm and 1,5 mm thick sheets had a nugget diameter of 4,9 mm. In order to find the correct nugget diameter, the spot welded samples were ripped apart and the nugget size was measured with a caliper. The measurements were only done on resistance spot welded beams (see table 3.5).

Table 3.5: The measured weld nugget diameter

Sheet thickness [mm]	1,0	1,5
Desired nugget diameter [mm]	4,0	4,9
Measured plug diameter [mm]	4,0 ± 0,1	5,0 ± 0,1

The desired nugget diameter was obtained with an electrode (cap), with a contact surface of 6 mm in diameter. Table 3.6 shows the settings of the robot for DP600 and Usibor.

Table 3.6: Welding parameters for DP600 and Usibor²

Steel	DP600	DP600	Usibor	Usibor
Thickness	1,0 mm	1,5 mm	1,0 mm	1,5 mm
Current	6,5 kA	6,7 kA	-	5,7 kA
Squeeze time	1000 ms	1000 ms	1000 ms	1000 ms
Welding time	270 ms	400 ms	270 ms	-
Electrode force	3,2 kN	4,4 kN	3,8 kN	4,9 kN
Cooling time	130 ms	150 ms	130 ms	150 ms

During the welding process excess adhesive squeezed out from the flanges. This indicated that the whole flange was filled with adhesive. After the welding process, excess adhesive was wiped off manually (see figure 3.8). Each beam was named with seven digits and each digit indicated a specific property. The extra beams (for calibration of the device) were marked with an E, meaning extra (see figure 3.9).



Figure 3.8: Wiping off the excess adhesive

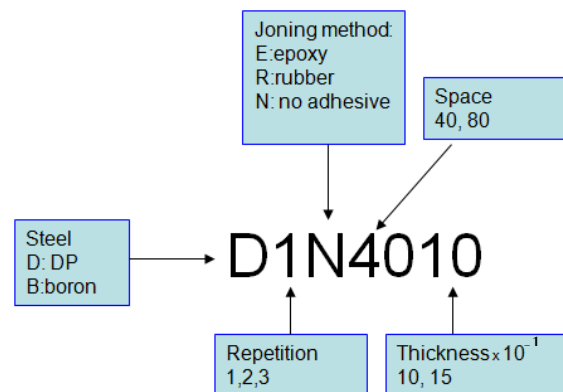


Figure 3.9: Nomenclature of the beams

3.3.2 Adhesive curing

The beams were put in a furnace for 45 minutes (200 °C) to cure the adhesive. The resistance spot welded beams were also put in the furnace, to ensure that all the beams had the same heat treatment.

3.4. 4-point bending in experimental tests

In the experimental test, the velocity was kept constant (10m/s) and two different masses (16,1 kg and 31,5 kg) were used. It was possible to obtain the velocities and deformations

² Some of the welding parameters are missing in this table.

(high and low) by changing the height. The relation between velocity and height are described by: (see equation 3.2 and 3.3)

$$E = mgh \quad \text{Potential energy} \quad (3.2)$$

$$E = \frac{mv^2}{2} \quad \text{Kinetic energy} \quad (3.3)$$

$$E = \text{energy} \quad [J]$$

$$m = \text{mass} \quad [kg]$$

$$v = \text{velocity} \quad [m/s]$$

$$h = \text{height} \quad [m]$$

$$g = \text{gravity} \quad [m/s^2]$$

All the tests were recorded by two high speed video cameras (2000 frames per second). Photos (1024x768 pixels) of the beams were taken after each 4-point bending test.

3.4.1 Measurements of deformation

In order to measure the static deformation of the beams, the beams were placed on a flat surface. The distance from the highest point of the hat profile to the flat surface was measured (see figure 3.10).

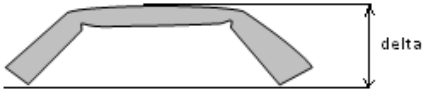


Figure 3.10: Measuring the maximum deformation of hat-lid beams (static).

Dynamic deformation was measured for all the beams. The dynamic deformation was measured by reviewing the test videos. The distance between the edge and the highest point of the hat profile was measured (see figure 3.11).

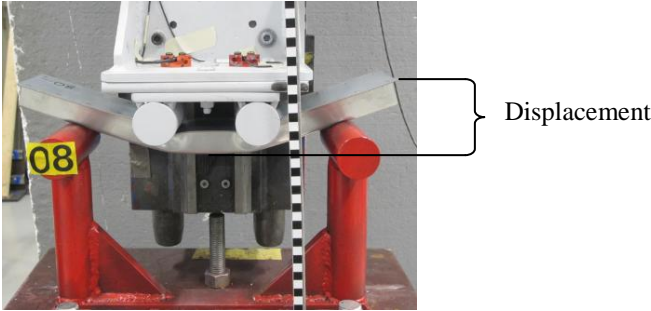


Figure 3.11: Measuring dynamic deformation

4. Results

This chapter presents the results of the CAE simulations and experimental tests. The test results from CAE simulations are dynamic results. The results from the experimental tests contain both dynamic and static results. The dynamic results are measured from the recorded test films and the static deformations are measured on the physical beam after the tests.

4.1 CAE Results of DP600 and Usibor

This chapter presents the results from the CAE simulations. It presents how the correct adhesive model was found, how the desired deformation was found and it also presents the result of 4-point bending.

4.1.1 Finding adhesive model in CAE

Rubber-based adhesive:

Usibor beams of 1,5 mm and 1,0 mm sheet thickness with 40 mm spot weld spacing were examined. The results showed no difference in deformation between weld bonded and spot welded beams, which means that the rubber adhesive model did not work properly. (The weld bonded beam should have a lower deformation than the resistance spot welded beam.)

Epoxy-based adhesive (type 1):

Usibor beams of 1,5mm sheet thickness with 40 mm spot weld spacing were examined. Three different adhesive models were tested (Model A, B and C). The results showed that the weld bonded beam had lower deformation than the resistance spot welded beam (the model worked properly). The segments were deleted with increasing deformation of the beam. The differences between the models were:

- Model A: stable, just a few segments were deleted.
- Model B: segments were deleted close to the hit point of the impactor.
- Model C: deleted segments to a larger extend than model B. The segments were deleted along the adhesive bond line (most realistic).

It was decided to use the model C in all the simulations, since it was the most realistic model. The beam in ANSA, was modeled with a mesh size of 2 mm. In order to investigate the influence of mesh size, the adhesive model was investigated with mesh sizes of 2 mm, 5 mm and 10 mm. The simulations were carried out for DP600 (thickness of 1,2 mm and 40 mm spot weld spacing, drop weight 40 kg and velocity 10m/s). The results showed that the deformation rates of the beams were the same, although different mesh sizes were used. A smaller mesh size showed higher sensitivity of the simulation model. In order to have accurate simulation results, it was decided to use 2 mm mesh size in all the simulations. Figure 4.1-4.3 shows the different mesh sizes in the 4-point bended beams.

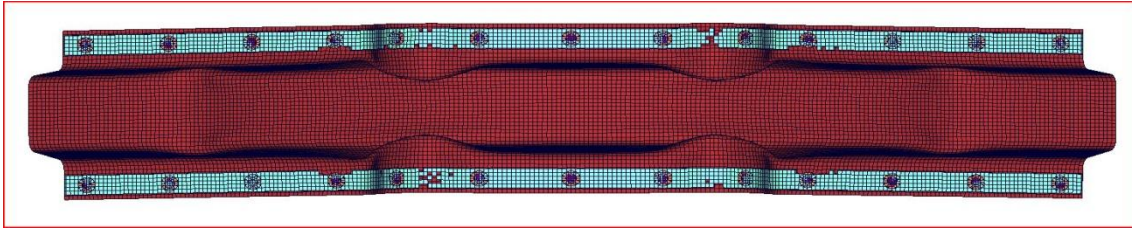


Figure 4.1: Adhesive mesh size of 2mm on the hat profile. Small segments were deleted.

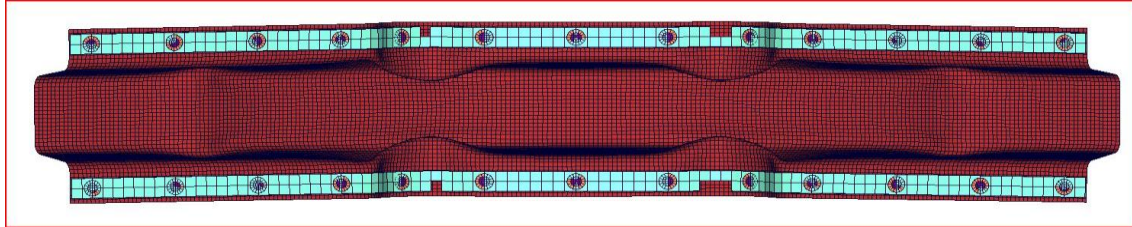


Figure 4.2: Adhesive mesh size of 5mm on the hat profile. Large segments were deleted.

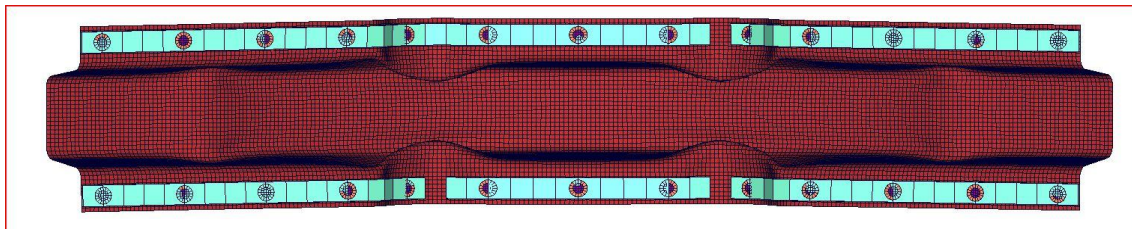


Figure 4.3: Adhesive mesh size of 10mm on the hat profile. Large segments were deleted and the sensitivity of the model was not accurate.

4.1.2 Finding desirable deformations in CAE

The simulation results showed that the steel cracked around the spot welds at 65 mm deformation. At 45 mm deformation the contribution of the adhesive was quite low for the Usibor beams. However, the contribution of adhesive was high in the DP600 beams at this deformation. The 65 mm deformation was decided to be the “high” deformation rate and 45 mm was decided to be the “low” deformation rate. The beams with 40 mm spot weld spacing without adhesive were used as the reference (see appendix 4).

4.1.3 Results of 4-point bending of DP600 in CAE

Figure 4.4 compares the deformation of spot welded beams with weld bonded beams. The values on the weld bonded bars show the deformation reduction in percent. It was of interest to compare the adhesive, sheet thickness and spot weld spacing of the beams. The appearance of the flanges was also of interest. The epoxy-based adhesive in this chapter is of type 1.

Comparing sheet thickness in DP600:

The reduction of deformation was higher in 1,0 mm sheet beams than in 1,5 mm sheet beams. For the 1,0 mm sheet beams, the reduction was 13,0% for 40 mm spot weld spacing and 15,3-22,6% for 80 mm spot weld spacing. For the 1,5 mm sheet beams, the reduction was 6,1-6,8% for 40 mm spot weld spacing and 12,5-14,6% for 80 mm spot weld spacing (see figure 4.4).

Comparing spot weld spacing in DP600:

The reduction of deformation was higher for 80 mm spot weld spacing than for 40 mm spot weld spacing. The percentage was 12,5%-22,6% for 80 mm spot weld spacing and 6,1%-13,0% for 40 mm spot weld spacing (see figure 4.4).

The highest reduction of deformation was gained at 80 mm spot weld spacing, with 1,0 mm sheet thickness. All the weld bonded beams had the same deformation. This was observed in both 40 mm and 80 mm spot weld spacing and at both 1,0 mm and 1,5 mm sheet thickness (see figure 4.4).

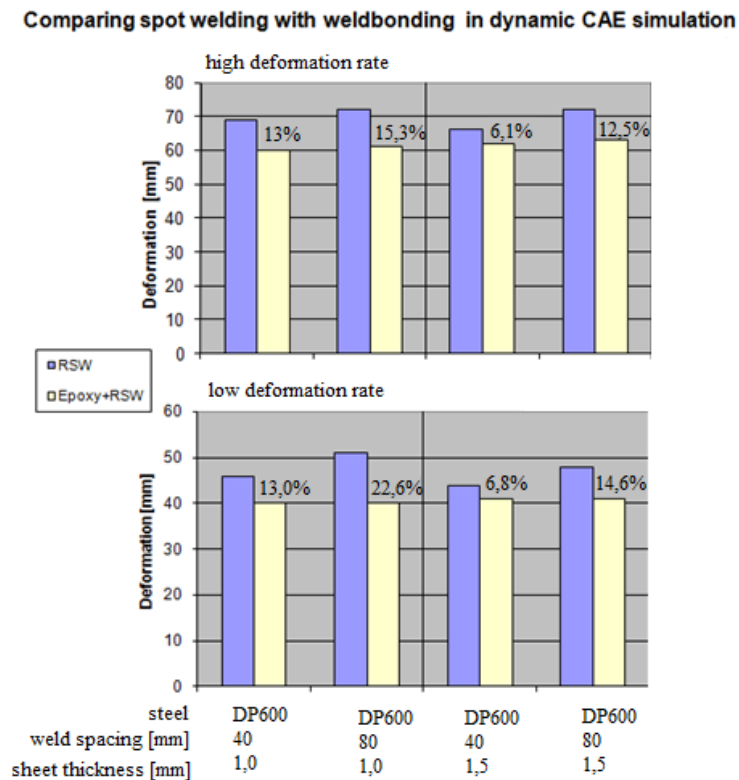


Figure 4.4: The numbers in percent shows how much less deformation the weld bonded beams had in comparison with the resistance spot welded beams.

4.1.4 Appearance of flanges DP600 beams

Many beams had similar failure modes and figure 4.5 shows the common failures. In 80 mm spot weld spacing the flanges separated in the resistance spot welded and weld bonded beams (see figure 4.5A). The flanges did not separate in 40 mm spot weld spacing (see figure Fig 4.5D), but there were small deletion of the adhesive segments in the weld bonded beams, similar to figure 4.5C. Table 4.1 lists the a detailed information for each beam.

Table 4.1: Description of the beams after 4-point bending

Sheet thickness	40 mm spot weld spacing	80 mm spot weld spacing
1,0 mm	<p>Resistance spot weld * No separation of flanges, spot welds were intact (see figure 4.5D).</p> <p>Epoxy weld bond * Small deletion of adhesive segments at the hit point of the impactor. Similar to figure 4.5B and 4.5C. * Similar appearance in high as in low deformation</p>	<p>Resistance spot weld * Separation of flanges, spot welds were intact. Similar to figure 4.5A.</p> <p>Epoxy weld bond * Small deletion of adhesive segments at the hit point of the impactor (see figure 4.5C). * Similar appearance in high as in low deformation</p>
1,5 mm	<p>Resistance spot weld * No separation of flanges, spot welds were intact (see figure 4.5D).</p> <p>Epoxy weld bond * Small deletion of adhesive segments along the adhesive bond line, similar to figure 4.5C. * High deformation rate had more adhesive deletion than low deformation rate.</p>	<p>Resistance spot weld * Separation of flanges, spot welds were intact. Similar to figure 4.5A.</p> <p>Epoxy weld bond * Deletion of adhesive segments along the adhesive bond line (see figure 4.5C). * High deformation rate had more adhesive deletion than low deformation rate. More deletion than the corresponding beam (1,0 mm beam with 80 mm spot weld spacing).</p>

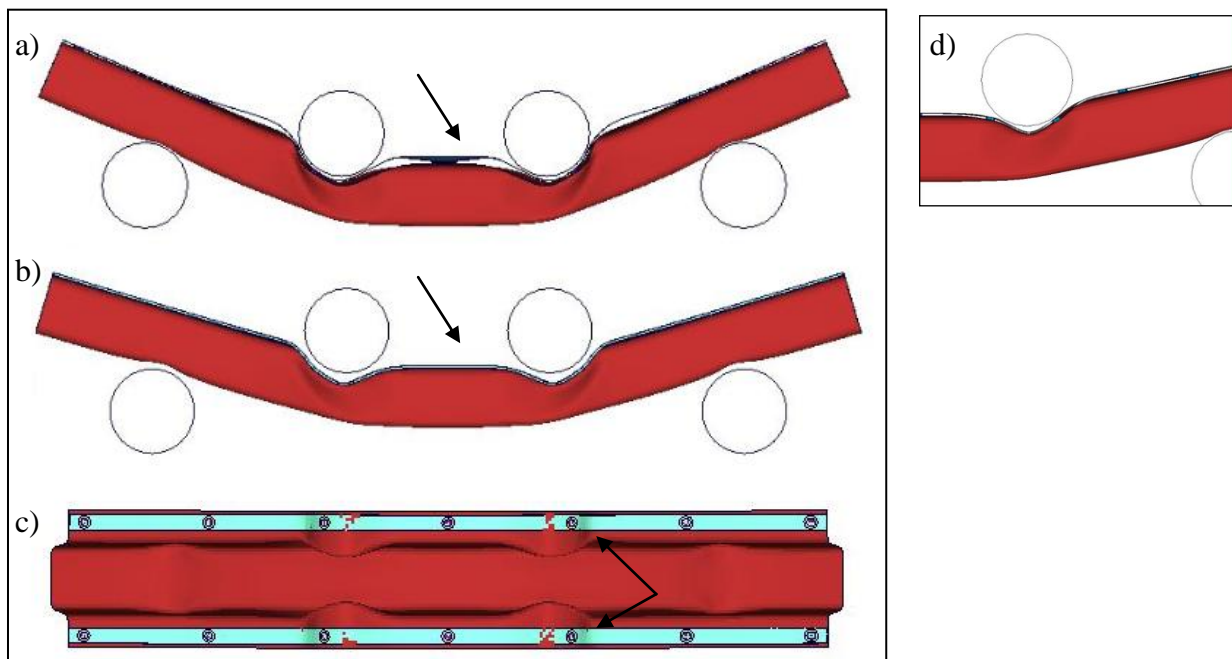


Figure 4.5: DP600 beam with thickness 1,0 mm and 80 mm spot weld spacing. The pictures show high deformation rate a) resistance spot welded beam with separation in the flanges b) weld bonded epoxy beam without separation c) adhesive failure at the hit points of the impactor on the hat profile. d) a resistance spot welded DP600 beam, with thickness 1,0 mm and 40 mm spacing. The flange follows nicely and the spot welds were intact.

4.1.5 Results of 4-point bending of Usibor in CAE

Figure 4.6 compares the deformation of spot welded beams with weld bonded beams. The value on the weld bonded bar shows the reduction of deformation in percent. The epoxy-based adhesive in this chapter is of type 1.

Comparing thickness in Usibor:

The reduction of deformation was higher in 1,0 mm sheet thickness than in 1,5 mm sheet thickness. It was 6,9%-9,1% deformation reduction for 1,0 mm sheet beams and 4,5%-8,9% deformation reduction for 1,5 mm sheet beams (see figure 4.6).

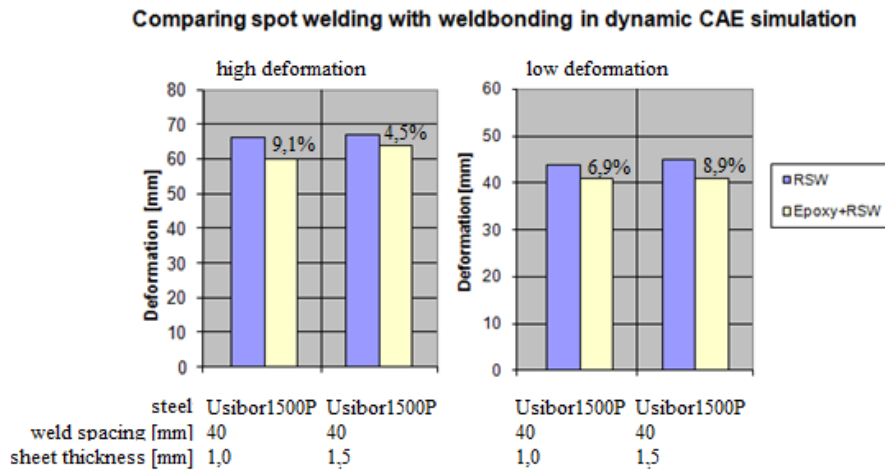


Figure 4.6: The numbers in percent show how much less deformation the weld bonded beam has in comparison with the resistance spot welded beam.

4.1.6 Appearance of flanges in Usibor beams

Figure 4.7 shows that the resistance spot welded beams had very small flange separation and the weld bonded beams had no flange separation (see figure 4.7A and figure 4.7B). The spot welds failed (close to the hit point of the impactor) in the resistance spot welded beams. Spot weld failure was prevented by the adhesive in the weld bonded beams, but a small amount of adhesive was deleted. In addition, no crack was found on the beams. Table 4.2 lists the detailed information for each beam.

Table 4.2. Description of the beams after 4-point bending

Sheet thickness	40 mm spot weld spacing
1,0 mm	<p>Resistance spot weld * Small separation of flanges, spot weld failure (4 spots close to impactor) (see figure 4.7A).</p> <p>Epoxy weld bond * Deletion of adhesive segments along the adhesive bond line Similar appearance in high as in low deformation (see figure 4.7B) * No separation of flanges (see figure 4.7B) * No crack in the steel</p>
1,5 mm	<p>Resistance spot weld * Small separation of flanges, the spot welds were intact in low deformation rate but failed at high deformation rate (see figure 4.7A).</p> <p>Epoxy weld bond * Small deletion of adhesive segments along the adhesive bond line (see figure 4.7B). High deformation rate had more adhesive deletion than low deformation rate. * No separation of flanges (see figure 2.7B) * No crack in the steel</p>

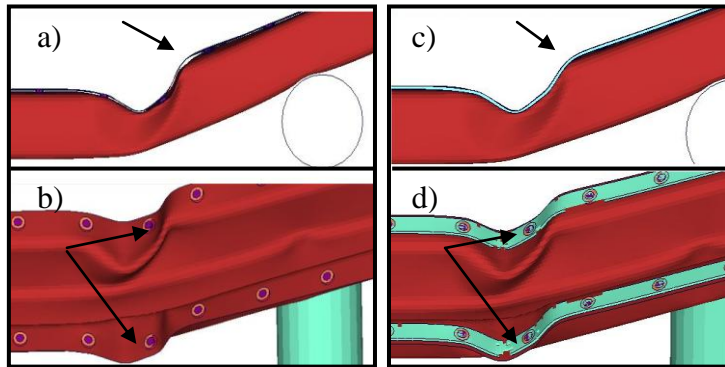


Figure 4.7: Usibor beams with 40 mm spot weld spacing, 1,0 mm sheet thickness and at high deformation rate. a) and b) resistance spot welded beams with spot failure c) and d) weld bonded beams with adhesive failure

4.1.7 Results of spring back

Table 4.3 shows the dynamic and static deformation of DP600 and Usibor beams. The spring back was calculated as the difference between dynamic deformation and static deformation. (The static deformation was obtained in CAE, by letting the simulations run for longer time.)

Table 4.3: Dynamic deformation and static deformation for beams with 1,0mm sheet thickness. The deformations were measured in Animator.

	DP600	Usibor
Dynamic deformation [mm]	41	43
Static deformation [mm]	36	31
Spring back [mm]	5	12

Higher spring back was expected for Usibor, since it had higher strength. Moreover, the cold

formed DP600 was expected to have less spring back, which was also observed in the simulations. Table 4.3 shows that Usibor had more than double the spring back compared to DP600.

4.1.8 Summary of CAE simulations

The simulations were carried out for DP600 and Usibor with different sheet thickness and spot weld spacing. All the CAE simulations were carried out with epoxy-based adhesive (type 1, the regular one), since the rubber-based adhesive model did not work (did not reduce deformation).

In general, the epoxy-based adhesive reduced the deformation more in DP600 than in Usibor. In the case for DP600 (for both thicknesses 1,0 mm and 1,5 mm), the reduction of deformation was higher in 80 mm spot weld spacing than in 40 mm spot weld spacing.

The reduction of deformation was higher in 1,0 mm sheet thickness, than in 1,5 mm. When comparing the reduction of deformation between low deformation rate and high deformation rate, it was observed that the influence of adhesive was higher at the low deformation rates. The adhesive started to lose its positive influence when it was exposed to high deformation rate due to over loading.

4.2 Experimental test results of DP600

In the experimental tests the weld bonded beams had either epoxy-based (type 2) or rubber-based adhesive in the flanges. Note that this epoxy-based (type 2) adhesive is not the same as the epoxy-based (type 1) adhesive mentioned in the CAE chapter.

The results of static deformation will be presented in the first part of this chapter, the second part will present dynamic deformation. The results will be presented for Usibor and DP600 beams in terms of separation, failure mode of adhesive and spot welds, material thickness, steel grade and spacing between spot welds (see appendix 5 and 6 for detailed comment on each test).

4.2.1 Comparing thickness and bonding of DP600

Figure 4.8 compares the deformation in spot welded beams with weld bonded beams. The values on the weld bonded bars show the reduction of deformation in percent. Each bar shows the average deformation of at least three tests.

Comparing sheet thickness in DP600 (rubber-based adhesive):

The reduction of deformation was higher in 1,0 mm sheet beams than in 1,5 mm sheet beams, this was observed for both 40 mm and 80 mm spot weld spacing. The reduction was 12,6%-29,3% for 1,0 mm thick beams. The reduction was 5,1%-15,6% for 1,5 mm thick beams (see figure 4.8).

Comparing spot weld spacing at the same thickness in DP600 (rubber-based adhesive):

The 1,0 mm beams with 80 mm spot weld spacing had high reduction of deformation (29,3 %) at low deformation rate. At high deformation rate the beams had 12,6% reduction, which means it was a large difference between high and low deformation rate for this test-setup . The reduction of deformation was 21,3%-25,5% for beams with 40 mm spacing (see figure 4.8).

The rubber weld bonded beams with 1,5 thickness had almost the same amount of deformation in both 40 mm and 80 mm spot weld spacing. The reduction of deformation was 11,4%-15,5% for 80 mm spot weld spacing and 5,1%-12,4% for 40 mm spacing (see figure 4.8).

Comparing rubber-based adhesive and epoxy-based adhesive:

The epoxy-based adhesive reduced the deformation more than the rubber-based adhesive, in DP600. The rubber-based adhesive reduced the deformation with 5,1%-12,4% and the epoxy-based adhesive reduced the deformation with 14,3%-15,6% (see figure 4.8).

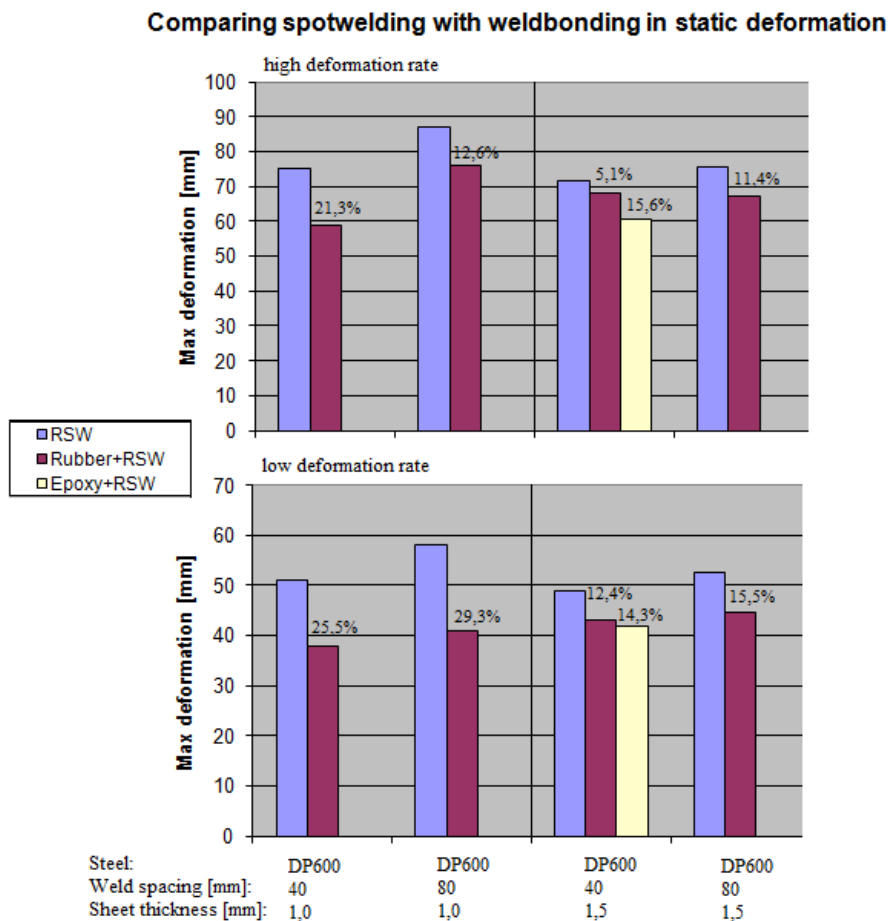


Figure 4.8: The deformations of spot welded and weld bonded beams at high and low deformation rates.

The difference in deformation, between 40 mm and 80 mm spot weld spacing was quite small for the resistance spot welded beams of 1,5 mm sheet thickness. The difference was only 4 mm (at both high and low deformation rate) (see figure 4.8).

4.2.2 Comparing the behavior of adhesive in DP600

Figure 4.9 shows the deformation vs. energy with sheet thickness 1,0 and 1,5mm. The results shows that the 1,5 mm beams can withstand higher energy than the 1,0 mm beams.

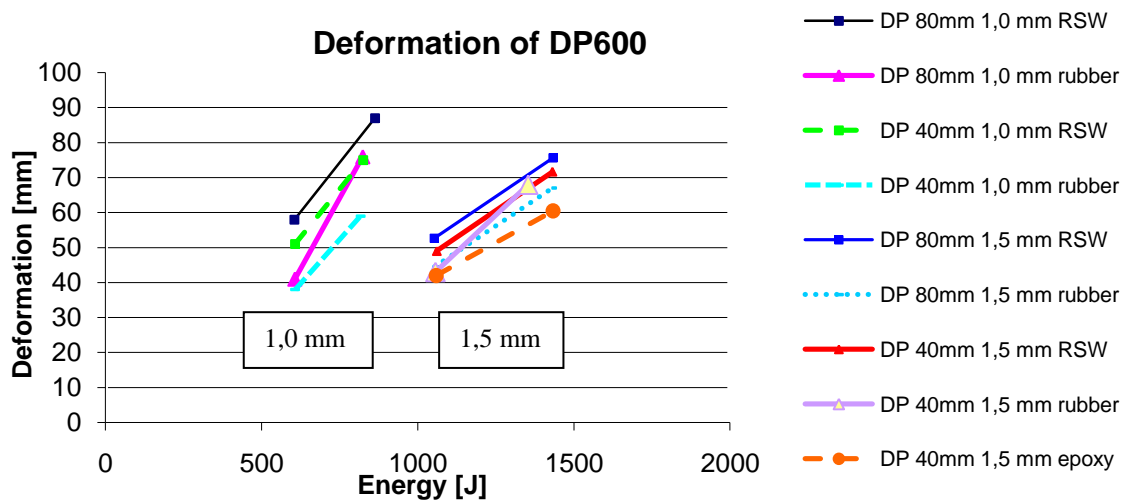


Figure 4.9. Thick sheet beams withstand higher energy than thin sheet beams

Figure 4.10 shows the trend of the adhesive behavior. It was observed that some weld bonded beams were “losing its effect” rapidly with increasing deformations. (The reduction of deformation was reducing rapidly with increasing deformation.)

Comparing spot weld spacing at 1,0 mm beams (rubber-based adhesive):

At 80 mm spot weld spacing, the reduction of deformation decreased with increasing deformation. The reduction decreased rapidly, because the load was too tough for the joint to withstand. At 40 mm spot weld spacing the reduction of deformation decreased slowly (with increasing deformation) (see figure 4.10).

Comparing spot weld spacing at 1,5 mm beams (rubber-based adhesive):

The rubber-based adhesive with 80 mm spot weld spacing had higher reduction of deformation than 40 mm spot weld spacing. This was because the 80 mm spot weld spacing “stretched” the adhesive. When the deformation increased (80mm spot weld spacing), the reduction of deformation decreased. The 80 mm spot weld spacing showed higher effect of adhesive than 40 mm. (see figure 4.10).

Comparing rubber and epoxy weld bonded beams:

When the deformation increased, the deformation reduction decreased for the rubber-based adhesive. The opposite behavior was observed for the epoxy-based adhesive. When the deformation increased, the reduction of deformation increased also. The epoxy-based adhesive was better than the rubber-based adhesive, because it could withstand higher deformation (see figure 4.10).

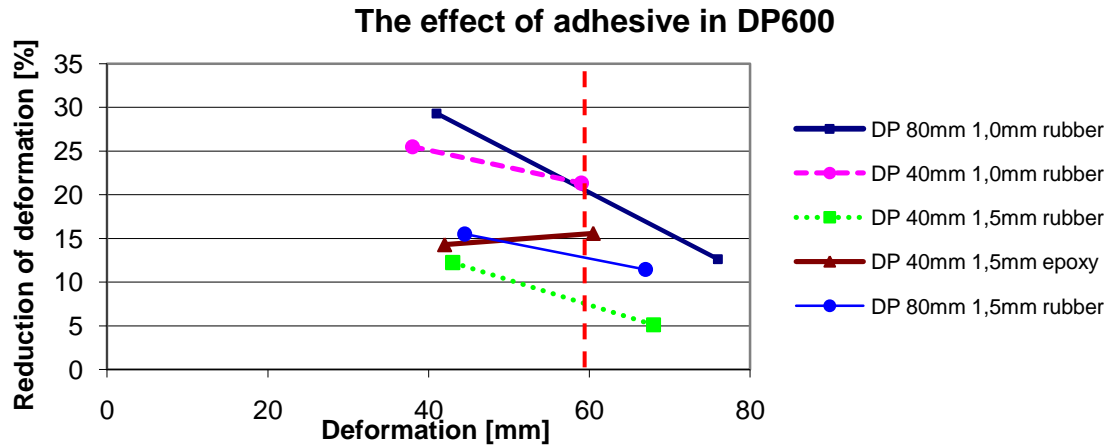


Figure 4.10: The graph shows (in percent) how much less deformation it is possible to obtain by the use of adhesive. The lines are drawn by using the values for high and low deformation rates. It is possible to see the trend of the adhesive behavior. It is possible to compare the beams at the same deformation, 60 mm.

In general, the 40 mm spacing showed higher effect of adhesive than 80 mm spacing (in 1,0 mm thick beams) and the epoxy-based adhesive was better than the rubber-based adhesive. Since it was difficult to obtain the exactly the same deformation in the experimental tests, the “high” and “low” deformation plots made it possible to compare all the beams at the same deformation.

- 80 mm spot weld spacing, 1,0 mm beams have 22,42% reduction with rubber adhesive
- 40 mm spot weld spacing, 1,0 mm beams have 21,13% reduction with rubber adhesive
- 40 mm spot weld spacing, 1,5 mm beams have 15,55% reduction with epoxy adhesive
- 80 mm spot weld spacing, 1,5 mm beams have 12,71% reduction with rubber adhesive
- 40 mm spot weld spacing, 1,5 mm beams have 7,40% reduction with rubber adhesive

With the information from the bullet points above it was be summarized that the highest reduction of deformation was observed at 1,0 mm thick beams. The 80 mm spot weld spacing had the highest reduction of deformation (low deformation rate), but the reduction was decreasing rapidly with higher deformations.

4.2.3 Appearance of flanges and spot welds in DP600 beams

The resistance spot welded beams and the weld bonded beams did not fail at the spot welds. The 1,0 mm and 1,5 mm thick beams presented good spot welds. It was only observed that the flanges separated between the spot welds. At close observations the 1,0 mm beams with 40 mm spot weld spacing had small deformations in the flanges (the flanges was starting to separate). It occurred at the hit points of the impactor of the resistance spot welded beams. The rubber weld bonded beams separated in the flanges and had cohesive failure of the adhesive. These observations were done at both high and low deformation rate (see figure 4.11-4.14).



Figure 4.11. DP600, 1,0 mm, 40 mm spot weld spacing, low deformation. From top: 3 RSW and 3 rubber weld bonded



Figure 4.12. DP600, 1,0 mm, 40 mm spot weld spacing, high deformation. From top: 3 RSW and 3 rubber weld bonded



Figure 4.13 The rubber adhesive starts to separate at the hit points of the impactor.



Figure 4.14 The rubber adhesive is still stable and no separation in the flanges was observed.

The resistance spot welded beams with 80 mm spacing, separated in the flanges at both high and low deformation rate (see figure 4.15-4.16). The flanges separated at the hit points of the impactor and the rubber-based adhesive failed cohesively. The flange separation in the rubber weld bonded beams was smaller than in the resistance spot welded ones. In general, the 80 mm spot weld spacing had more separation in the flanges than 40 mm spacing (see figure 4.17-4.18).



Figure 4.15: DP600, 1,0 mm, 80mm spot weld spacing, low deformation. From top: 2 RSW and 2 rubber weld bonded



Figure 4.16: DP600, 1,0 mm, 80mm spot weld spacing, high deformation. From top: 3 RSW and 2 rubber weld bonded



Figure 4.17: Magnified picture of the separation at low deformation. From top: RSW and rubber weld bonded.



Figure 4.18: The RSW-beams separate more than rubber weld bonded beams at high deformation. From top: RSW and rubber weld bonded.

The separation in the flanges of the 1,5 mm beams with 40 mm spot weld spacing was small. The resistance spot welded and rubber weld bonded beams started to separate in the flanges. The epoxy weld bonded beams did not show any separations. Figure 4.19-4.20 show that the flanges had very small separations. Figure 4.21-4.22 show magnified photos of the separations.



Figure 4.19: DP600, 1,5 mm thick, 40 mm spot weld spacing, low deformation. From top: 3 RSW, 2 rubber and 2 epoxy weld bonded.



Figure 4.20: DP600, 1,5 mm thick, 40 mm spot weld spacing, high deformation. From top: 3 RSW, 2 rubber and 2 epoxy weld bonded.

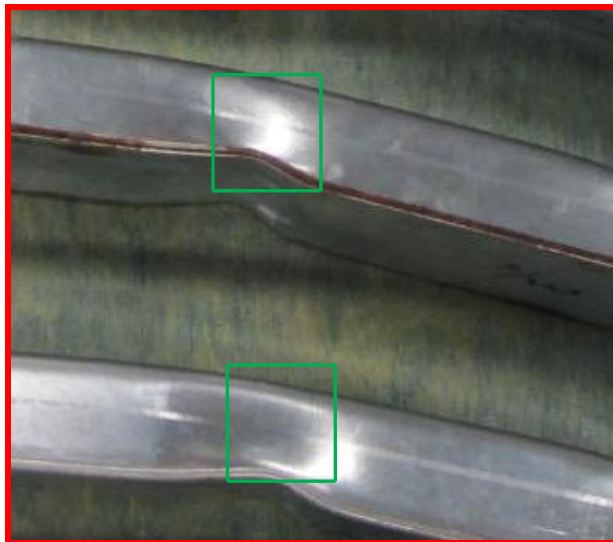


Figure 4.21: The green square at the top show that rubber adhesive starts to fail cohesively, whereas epoxy adhesive below show no separation.

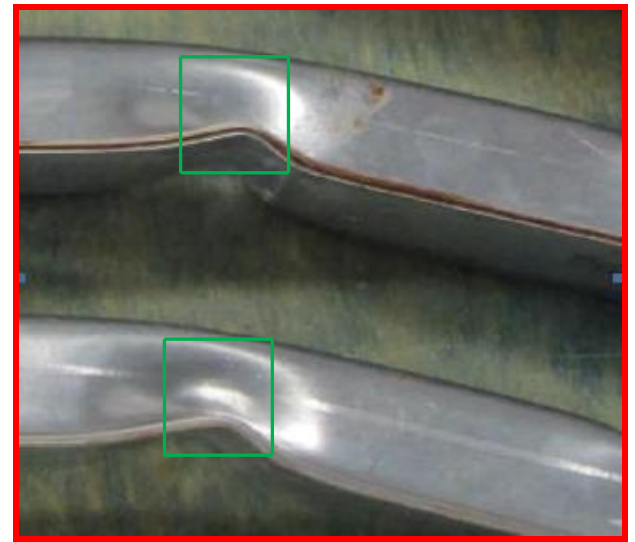


Figure 4.22: The green square at the top show that rubber adhesive starts to fail cohesively, whereas epoxy adhesive below show no separation.

Figure 4.23-4.24 shows the beams of 1,5 mm thickness with 80 mm spot weld spacing. It was observed that the beams separated in the flanges at both high and low deformation rate. The rubber weld bonded beams did not prevent separation and it also failed cohesively.



Figure 4.23: DP600, 1,5 mm thick, 80 mm spot weld spacing, low deformation. From top: 3 RSW and 2 rubber weld bonded.



Figure 4.24 : DP600, 1,5 mm thick, 80 mm spot weld spacing, high deformation. From top: 3 RSW and 2 rubber weld bonded.

Comparing the flanges in DP600 beams:

In 40 mm spot weld spacing both 1,0 mm and 1,5 mm beams had small separations of the flanges. In 80 mm spot weld spacing both 1,0 mm and 1,5 mm had larger separation of the flanges. There was no significant difference in flange separation between thickness 1,0 mm and 1,5 mm (see figure 4.25-4-26).

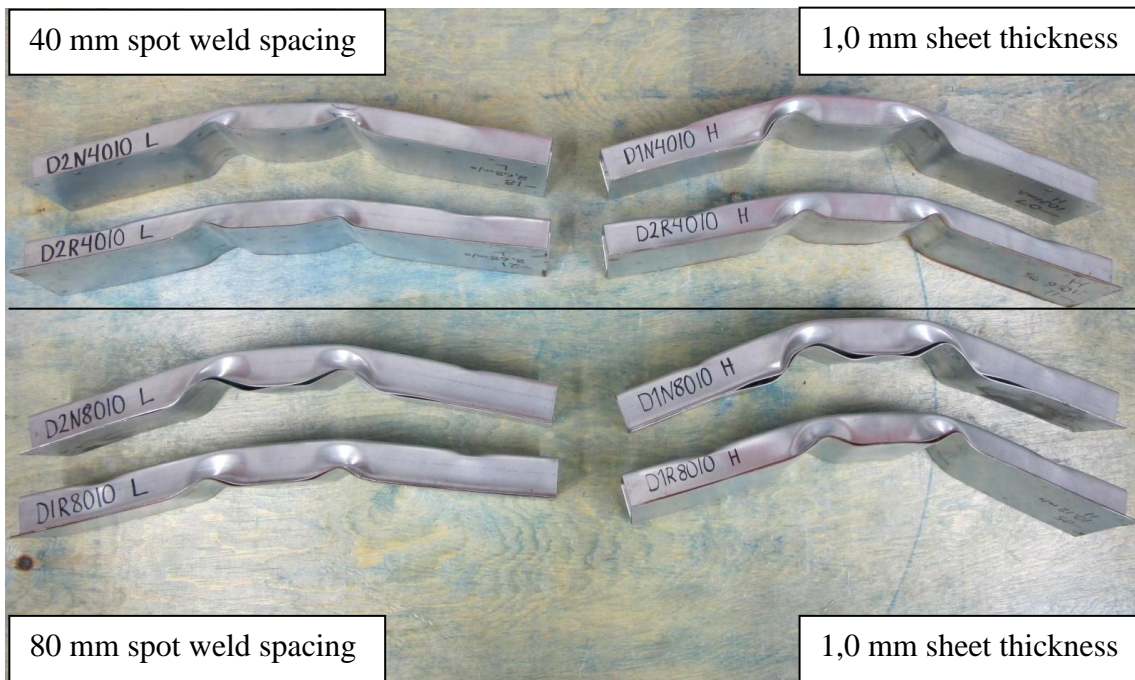


Figure 4.25: All the beams in the picture are in sheet thickness 1,0 mm. The upper part is showing 40 mm spot weld spacing and the lower part is showing 80 mm spacing. The beams are positioned in pair. From top: RSW and rubber weld bonded.

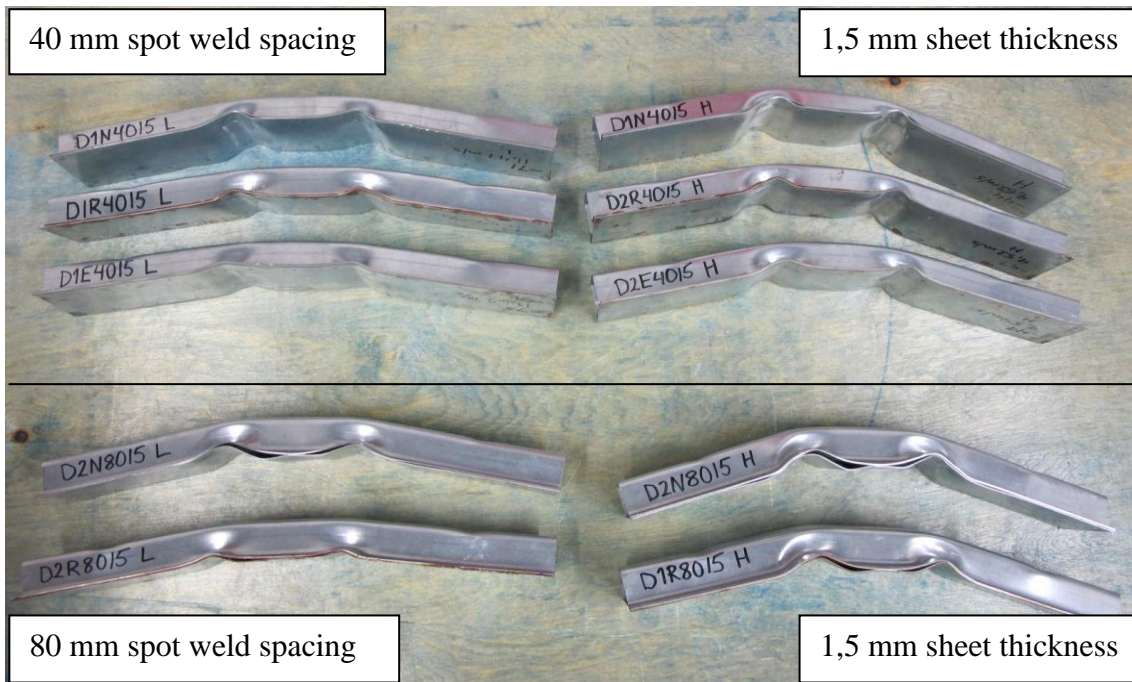


Figure 4.26: All the beams in the picture are in sheet thickness 1,5 mm. The upper part is showing 40 mm spot weld spacing and the beams are grouped. From top: RSW, rubber weld bonded, epoxy weld bonded. The lower part of the picture is showing 80 mm spot weld spacing. The beams are positioned in pairs. From top: RSW and rubber weld bonded.

4.3 Experimental test results of Usibor

The results show the max static deformation. The epoxy-based adhesive (type 2) in this chapter is especially developed for press-hardened steel.

4.3.1 Comparing thickness and bonding of Usibor

Figure 4.27 compares the deformation in spot welded beams with weld bonded beams. The value on the weld bonded bars show the reduction of deformation in percent. Each bar shows the average deformation of at least three tests.

Comparing sheet thickness in Usibor (rubber-based and epoxy-based adhesive):

The weld bonded beams had higher deformation than the just resistance spot welded beam (at high deformation rate). The rubber weld bonded (1,0 mm beams) had 10,4% higher deformation than the just spot welded beams. The epoxy weld bonded beams (1,0 mm beam) had 9,1% higher deformation than the spot welded beams (negative percent) (see figure 4.27)

The reduction of deformation was low in the 1,0 mm beams at low deformation rate. At low deformation rate, the reduction of deformation was almost the same for both rubber and epoxy weld bonded beams. The reduction of adhesive was more visible in the 1,5 mm thick beams. The contribution of adhesive was 4,1%-7,6% (see figure 4.27).

Comparing rubber adhesive and epoxy adhesive:

The epoxy-based adhesive and rubber-based adhesive reduced the deformation in low amounts in Usibor. The rubber-based adhesive reduced the deformation with 5,1% and the epoxy adhesive with 3,7 % (at low deformation rate) (see figure 4.27).

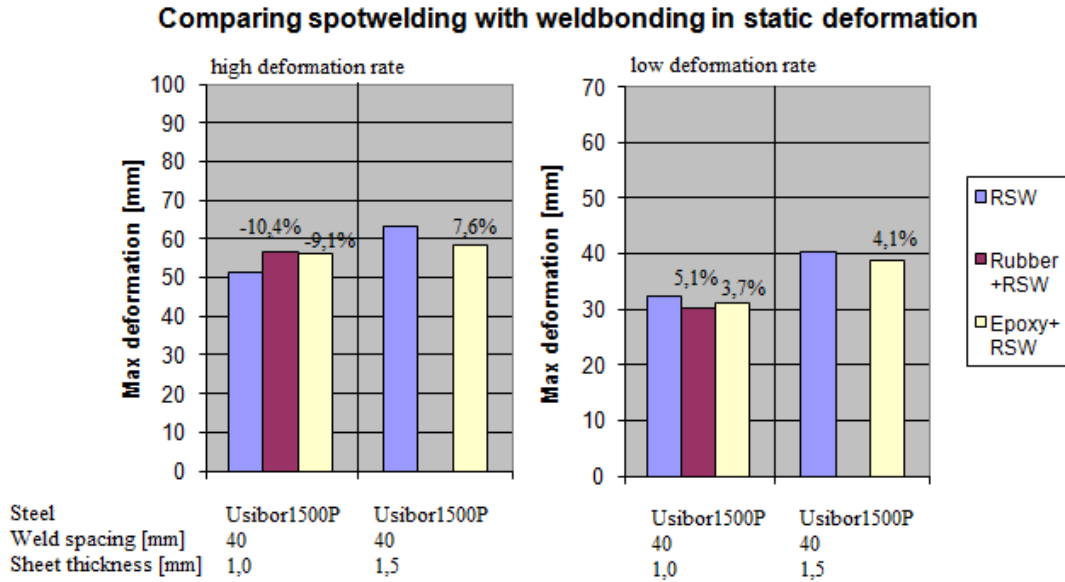


Figure 4.27: The deformations of spot welded and weld bonded beams at high and low deformation rates.

4.3.2 Comparing the behavior of adhesive in Usibor

Figure 4.28 shows the deformation vs. energy for Usibor with thickness 1,0 mm and 1,5 mm. The results show that 1,5 mm beams can withstand higher energy than 1,0 mm beams.

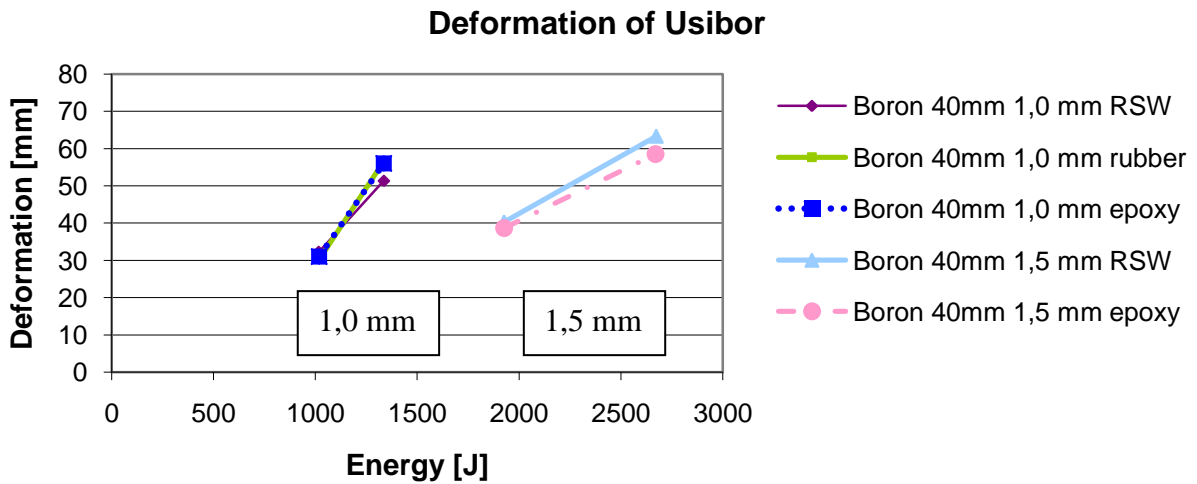


Figure 4.28: Thick sheet beams can withstand higher energy than thin sheet beams.

Figure 4.29 shows the trend of the adhesive behavior. It was observed that some of the weld bonded beams were “losing its effect” rapidly with increasing deformations. (The reduction of deformation was reduced rapidly with increasing deformation.)

Comparing rubber and epoxy weld bonded beams:

The rubber-based and epoxy-based adhesive were losing their effect rapidly in the 1,0 mm thick beams. The weld bonded beams (rubber and epoxy) had higher deformation than resistant spot welded beams (see figure 4.29). (The reduction of deformation was negative, when rubber-based and epoxy-based adhesive was used in the flange.)

The following behavior was only observed for the 1,5 mm thick beams. The reduction of deformation (epoxy-based adhesive) was increasing from low to high deformation rate. At low deformation it was only 4% and at high deformation the value was 7%. The 1,0 mm sheet thickness showed the opposite behavior. The reduction of deformation was decreasing with higher deformations (see figure 4.29).

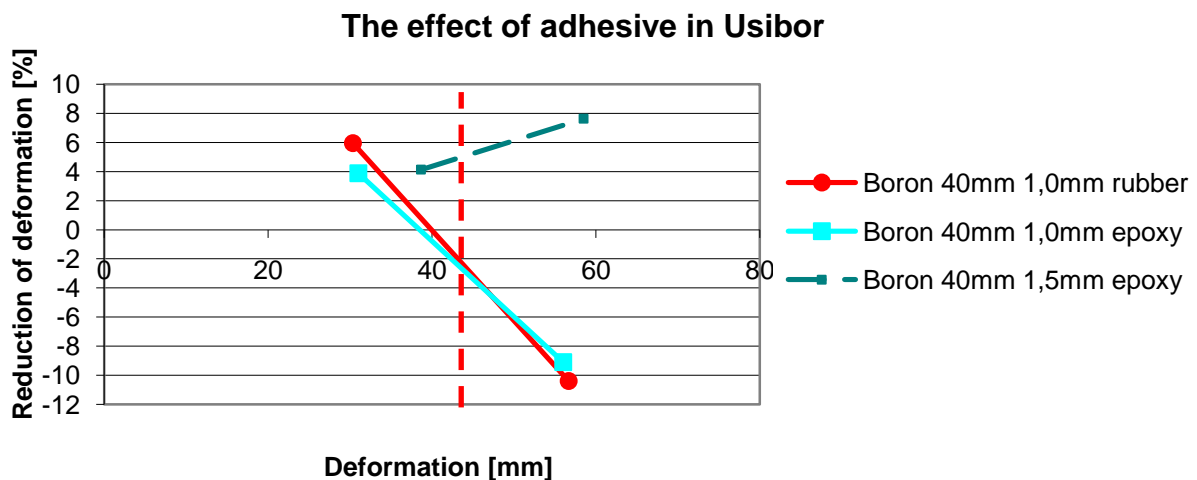


Figure 4.29: The graph shows (in percent) how much less deformation it is possible to obtain by the use of adhesive. The lines are drawn by using the values for high and low deformation rates. It is possible to see the trend of the adhesive behavior. It is possible to compare the beams at the same deformation, 45 mm.

The “high” and “low” deformation graphs made it possible to compare all the beams at the same deformation. All the Usibor beams (resistance spot welded, rubber weld bonded, epoxy weld bonded) were compared at 45 mm deformation. Figure 4.29 shows these values at the same deformation:

- 40 mm spot weld spacing, 1,0 mm beams have 3,22% higher deformation than the RSW with rubber-based adhesive
- 40 mm spot weld spacing, 1,0 mm beams have 3,45% higher deformation than the RSW with epoxy-based adhesive
- 40 mm spot weld spacing, 1,5 mm beams have 5,24% lower deformation than the RSW with epoxy-based adhesive

With the information from the bullet points above it was be summarized that the weld bonded 1,0 mm thick beams with 40 mm spot weld spacing had higher deformation than the just resistance spot welded beams (the percentage was negative).

4.3.3 Appearance of flanges and spot weld in Usibor beams

The Usibor beams (RSW, rubber and epoxy weld bonded) separated in the flanges. The rubber weld bonded beams had larger separation in the flanges than the resistance spot welded beams. The green squares in figure 4.30-4.31 shows that the rubber-based adhesive had the largest separation than of all the beams. The rubber-based adhesive failed cohesively in both sheet thicknesses and both sides of the adherent had remaining adhesive (see appendix 5 and 6). Figure 4.32-4.33 shows the beams in 1,5 mm sheet thickness.



Figure 4.30: Usibor, 1,0 mm thick, 40 mm spot weld spacing, low deformation. From top: 3 RSW, 3 rubber weld bonded and 3 epoxy weld bonded.



Figure 4.31: Usibor, 1,0 mm thick, 40 mm spot weld spacing, high deformation. From top: 3 RSW, 3 rubber weld bonded and 3 epoxy weld bonded.



Figure 4.32: Usibor, 1,5 mm thick, 40 mm spot weld spacing, low deformation. From top: 5 RSW and 3 epoxy weld bonded.



Figure 4.33: Usibor, 1,5 mm thick, 40 mm spot weld spacing, high deformation. From top: 3 RSW, 3 rubber and 3 epoxy weld bonded.

Figure 4.34-4.35 show that the separation was larger for the weld bonded (epoxy and rubber) beams than the just resistance spot welded beams. The epoxy did not prevent separation of the flanges. It was observed that the surface was shiny on one side of the flange. On the surface of the other side, there was a grey dull layer which was the coating of the Usibor. The Al-Si coating of the steel was ripped off by the adhesive. This surface coating delamination

occurred at both the 1,0 mm and 1,5 mm beams. Figure 4.34-4.375 show magnified photos of the adhesive failures. The rubber weld bonded beams had larger separation in the flanges than the resistance spot welded beams.



Figure 4.34: Usibor, 1,0 mm thick, 40 mm spot weld spacing, low deformation. From the top: RSW, rubber weld bonded and epoxy weld bonded.



Figure 4.35: Usibor, 1,0 mm thick, 40 mm spot weld spacing, high deformation. From the top: RSW, rubber weld bonded and epoxy weld bonded.

Figure 4.36-4.37 shows different failures in a resistance spot welded 1,5 mm beams. The spot welds failed in two different modes, some spot welds failed by plug failure and others by interfacial fracture. The plug failure is shown in the square to the right in figure 4.36. The left square in figure 4.36 shows an interfacial fracture. The Usibor beams had a small crack (in millimeter range) in the hat profile. Almost all the resistance spot welded, rubber and epoxy weld bonded beams had this failure (see figure 4.37).

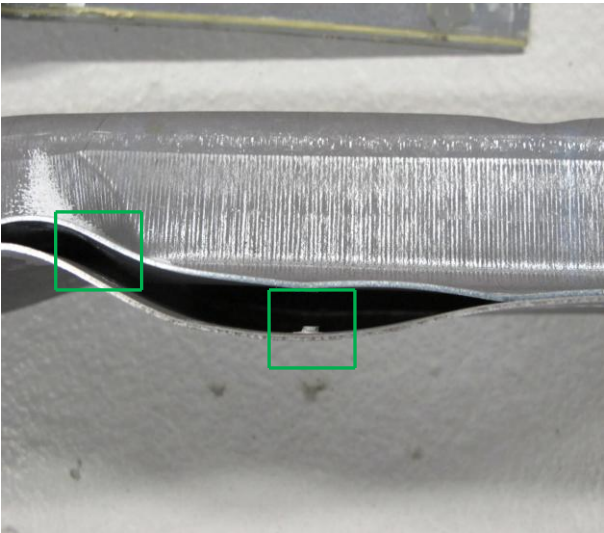


Figure 4.36: The squares are showing two different spot weld failures, plug failure (right) and interfacial failure (left).

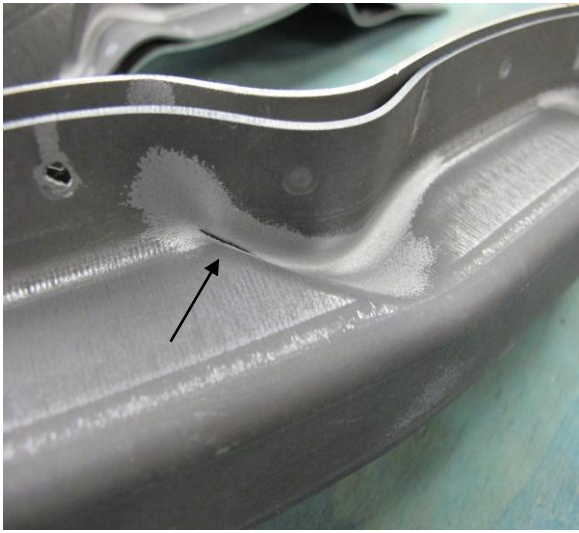


Figure 4.37: Crack in the hat profile at the hit point of the impactor.

Comparing the flanges in Usibor:

In 1,0 mm thickness, the rubber weld bonded beams had higher deformation than the resistance spot welded ones. The epoxy weld bonded beams had almost the same deformation as the resistance spot welded beams. The epoxy-based adhesive did not have a very distinct effect on separation and deformation reduction. It was also observed that the 1,0 mm beams had less separation (less number of spot weld failures) in the flanges than the 1,5 mm beams (see figure 4.38-4.39).



Figure 4.38: Usibor beams with thickness 1,0 mm. From top: RSW, rubber weld bonded and epoxy weld bonded, both high (upper group) and deformation (lower group)

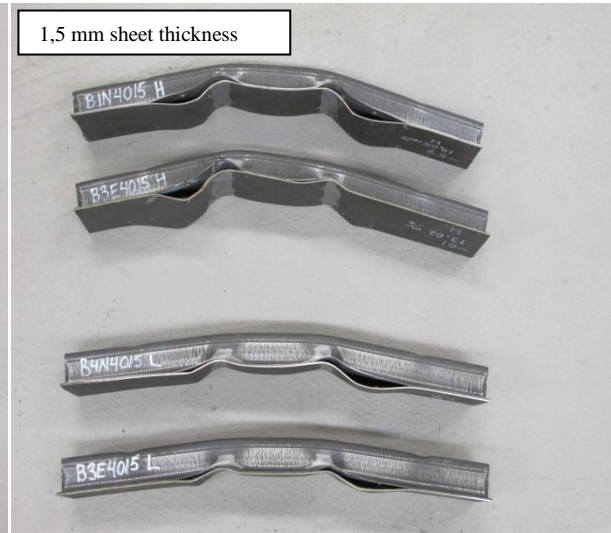


Figure 4.39: Usibor beam with thickness 1,5 mm. From top: RSW and epoxy weld bonded for high (upper group) and low (lower group) deformation.

4.4 Scatter of deformation

Figure 4.40 shows the scatter of the measured deformation of the beams. Each point represents a tested beam. Some of the beams were missing in this graph, since the velocity was not measured successfully. Each test setup (with different mass and velocity) was performed in 2-5 repetitions (extra beams counted into the tests).

- The scatter was quite small in DP600, the deformation was similar in each repetition. (Except for one of the resistance spot welded beam, which is test marked with a square in the figure 4.40. This RSW point has correct input values such as velocity and mass.)
- There was a large scatter of the rubber weld bonded and epoxy weld bonded beams in Usibor of 1,0 mm sheet thickness. However, the RSW-points within the same group had small scatter.
- There was a large scatter among the RSW specimen in Usibor with 1,5 mm thickness, but the weld bonded epoxy beams within this group had smaller scatter.

With the information from the bullet points above, it was summarized that the DP600 beams had repetitive result, but the results of Usibor varied for each test (see figure 4.40). Similar results were observed at low deformation.

The measured static deformation

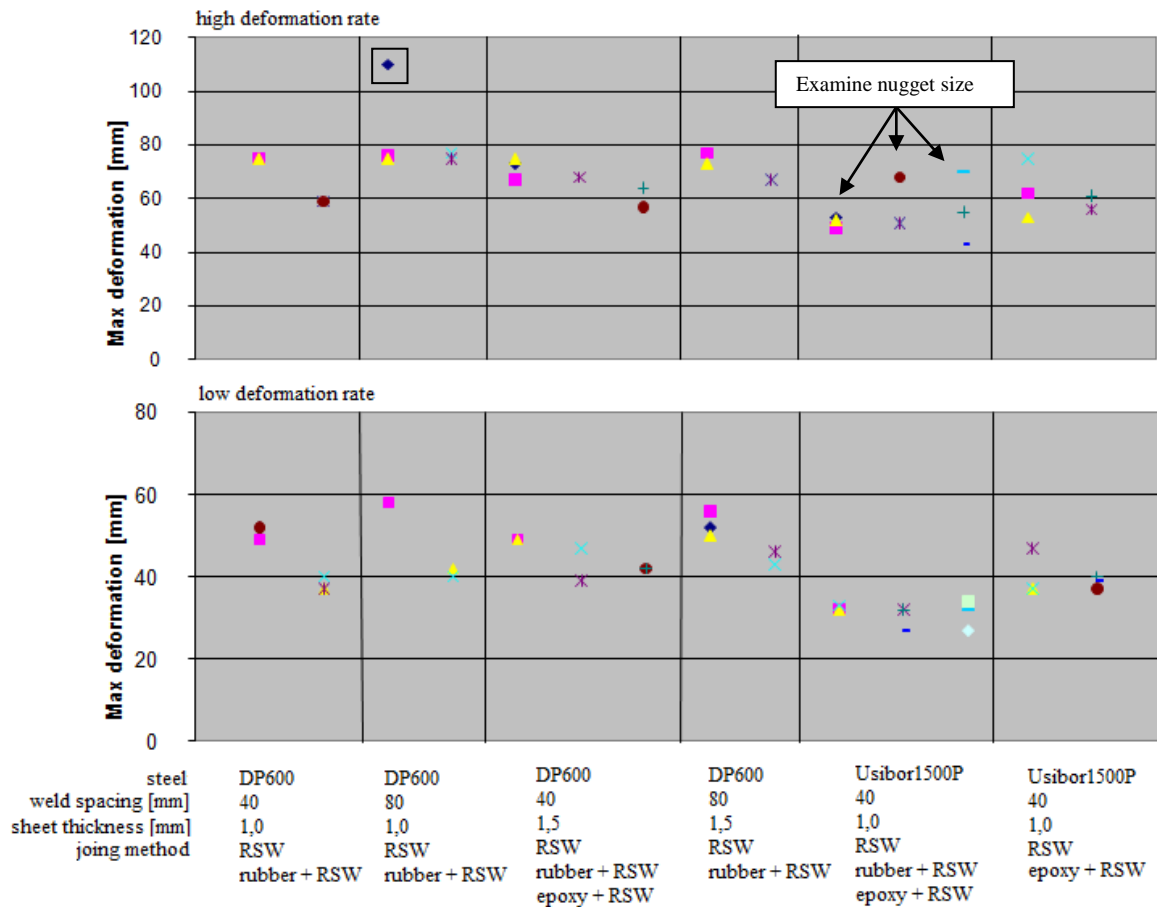


Figure 4.40: The graph shows the measured deformation for each test.

Figure 4.40 marks the three beams which were selected for nugget size measurement. These beams were examined since their deformations were deviating from other tests. The nugget sizes were almost the same in the three beams. The obtained nugget diameters were: 4,24 mm for the just resistance spot welded beams, 4,29 mm for the rubber bonded beam and 4,16 mm for the epoxy weld bonded beam (see appendix 8 for cross section pictures of the weld nugget). All the nugget sizes were in the correct range.

4.5 Summary of the experimental tests (static deformation)

In general, the adhesive reduced the deformation more in DP600 than in Usibor. Both rubber-based and epoxy-based adhesives (type 2) reduced separation of flanges in DP600 beams. The flanges separated more in 80 mm spot weld spacing than in 40 mm (DP600 beams).

The weld bonded Usibor beams had bigger flange separation than the resistance spot welded beams. The rubber-based adhesive failed cohesively and the epoxy-based adhesive (type 2) caused surface delamination of the Al-Si surface coating. It was also observed that the 1,5 mm sheet thickness had bigger flange separation than the 1,0 mm sheet thickness. The adhesive did not prevent spot weld failure in the flanges (Usibor beams) and a small crack was found in the hat profile in both thicknesses.

4.6 Dynamic deformation

Dynamic deformation was obtained by measuring the deformation from the test films (during the hitting moment). This chapter presents a short analysis of the dynamic deformation, since some of the data were missing (due to camera problems and failing of measuring acceleration). The dynamic results showed higher deformation than static deformation, because the dynamic deformation did not have any spring back of the beam.

Figure 4.41 shows the dynamic deformation. The rubber-based adhesive reduces the deformation more in DP600 than in Usibor. The reduction of deformation in DP600 was between 7,3% to 20,9% with rubber-based adhesive.

The reduction of deformation (with epoxy-based adhesive) was 7,3% to 16% in Usibor (at low deformation rate). At high deformation rate the epoxy weld bonded and rubber weld bonded beam had higher deformation than the resistance spot welded beams (sheet thickness 1,0 mm). In general, the epoxy-based adhesive was better than the rubber-based adhesive. The epoxy-based adhesive had higher reduction of deformation than the rubber-based adhesive in both DP600 and Usibor. Figure 4.42 shows the scatter of the measured deformations. In all the tests the scatter was quite small. The DP600 and Usibor beams had small scatter.

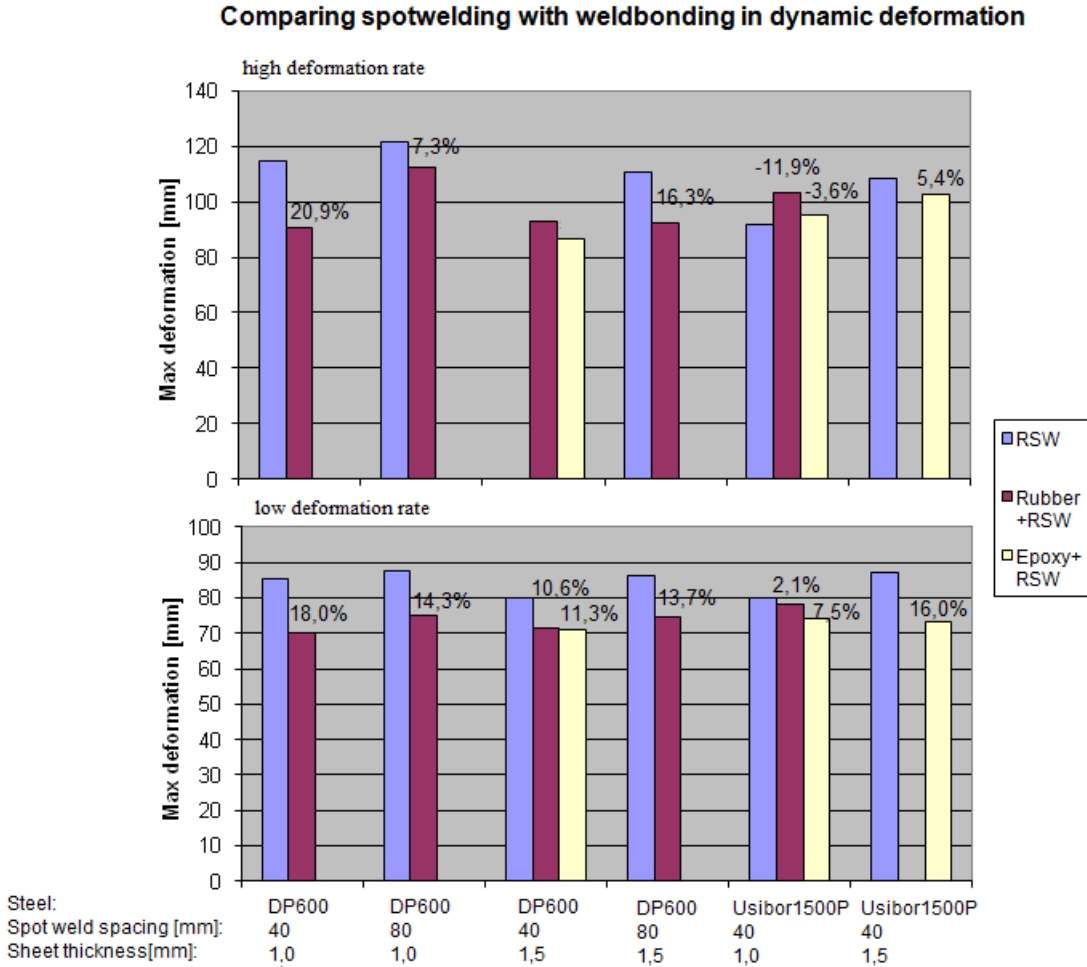


Figure 4.41: The deformations of spot welded and weld bonded beams at high and low deformation rates.

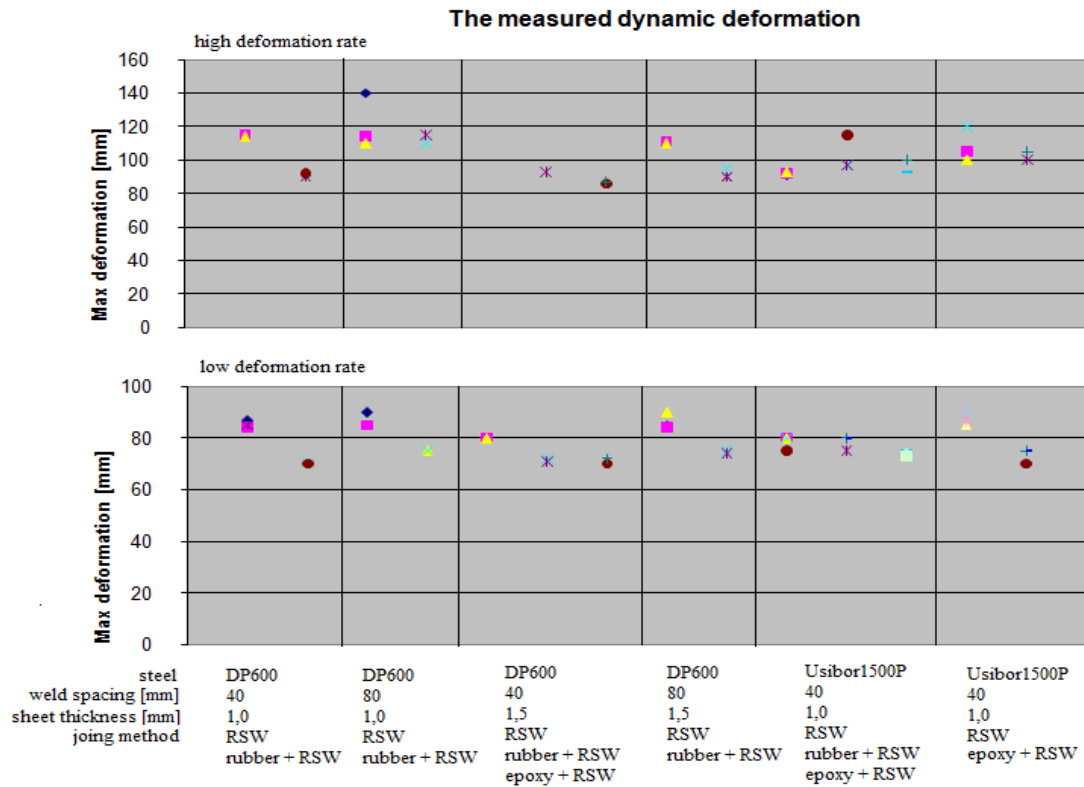


Figure 4.42: The graph is showing the spread of deformation of 4-point bended beams at high deformation rate.

4.6.1 Comparing dynamic deformation with static deformation

The spring back was obtained by measuring the difference between dynamic and static deformation. DP600 had spring back values of 23-40 mm and Usibor had spring back values of 23-53mm. These measurements were made on spot welded and weld bonded beams at 40 mm spot weld spacing. These results match with the results from the simulations. Usibor had more spring back than DP600. The values of the spring back for dynamic and static deformation from the experimental tests can be found in appendix 5.

The dynamic results of DP600 and Usibor showed that the beams had (almost) the same deformation in all the repetitions (see figure 4.42). However, the static results of Usibor had large scatter of deformation (see figure 4.40).

4.7 Correlation between CAE simulations and experimental tests

The adhesive was reducing deformation and preventing separation of the flanges in the CAE simulations. In the experimental tests (both rubber-based and epoxy-based) adhesives was reducing deformation and flange separation in DP600. However, in the case of Usibor, the weld bonded beams had surprisingly bigger flange separation than the just resistance spot welded beams and the adhesive did not reduce the deformation in some cases.

In the experimental tests, the Usibor beams had spot weld failure and the adhesive did not prevent spot weld failure in the flanges. These results correspond well to the CAE simulation results. Both 1,0 mm and 1,5 mm thick Usibor beams had small crack in the hat profile in the experimental tests and this did not correspond to the CAE results.

5. Discussion

The CAE results showed that the adhesives reduced the deformation of the beams and also the separation of the flanges. The experimental results showed similar results, but the epoxy-based and rubber-based adhesive reduced the deformation and flange separation in DP600-beams only. The adhesives could not prevent spot failure and flange separation in Usibor beams (in the experimental tests). The weld bonded beams had either the same (or higher) amount of flange separation than the resistance spot welded beams.

The DP-beams (in the experimental tests, with 80 mm spot weld spacing and 1,0 mm sheet thickness), was losing the effect of adhesive rapidly, because the load was too tough for the joint. The effect of the adhesive was decreasing slowly in 40 mm spot weld spacing, because the weld was not overloaded as in 80 mm spot weld spacing. It was also observed that the contribution of adhesive was more visible in thin DP600 sheet beams than thick sheet beams. When the rubber weld bonded beam failed, the adhesive failed cohesively because the adhesive was weak.

The CAE results of Usibor did not correspond well with the experimental tests. The beams had less number of failed spot welds in the simulations (Usibor), than in the experimental tests. In addition, all the beams (even in low level deformation) cracked in the hat profile in the experimental tests, but not in the CAE simulation. It might not be possible to compare the CAE results with experimental results, because two different adhesives were used. Epoxy-based adhesive type 1, was used in the CAE simulations and epoxy-based adhesive type 2 was used in the experimental tests.

The experimental test results showed that the thin Usibor beams (1,0 mm thick with 40 mm spot weld spacing) were losing the effect of adhesive with increasing deformation, but the thick (1,5 mm sheet) beams were showing the opposite effect. The contribution of the adhesive was increasing with higher deformation in thick beams. The reason might be that the (1,5mm sheet) beams were thick and stiff, which prevented the adhesive to become “overloaded”. It was also observed that the Al-Si coating (Usibor in experimental test) was removed from the steel by the epoxy-based adhesive. The coating removal was due to the powerful properties of the epoxy-based adhesive and the weak surface coating of the Usibor. Due to surface delamination, the epoxy-based adhesive could not reduce deformation and prevent flange separation of the beams.

The CAE results and experimental results corresponded well to the hypothesis. The beams failed in the spot weld and thick sheet beams could withstand higher forces than thin sheet beams. As expected, the results showed that the long spot weld spacing (80 mm) could withstand less energy compared to short spot weld spacing (40 mm).

6. Conclusions

The adhesive model for rubber-based adhesive did not correlate with experimental test results. However, the adhesive model for epoxy-based adhesive (type 1) correlated well.

The CAE results of DP600 correlated well with the results in the experimental tests. The epoxy-and rubber weld bonded beams had less deformation than the just resistance spot welded beams. The adhesives reduced the deformation of the beams.

The CAE results of Usibor did not correlate with the results of the experimental tests. Weld bonded Usibor beams had higher flange separation than the resistance spot welded beams in the experimental tests. This was not observed in the CAE results.

The adhesives (rubber-based and epoxy-based) reduced the deformation of DP600 beams in the experimental tests. In general, adhesive bonded DP600 beams had less flange separation than the just resistance spot welded beams. When the rubber adhesive failed in DP600 beams, they failed cohesively. The epoxy-based adhesive (type 2) did not fail in the DP600 beams.

The contribution of rubber adhesive was higher in 1,0 mm beams than in 1,5 mm DP600 beams. The beams with 40 mm spot weld spacing had high contribution of adhesive (1,0 mm thick sheet beams). At 80 mm spot weld spacing the rubber-based adhesive stretched too much and the adhesive lost its effect.

Adhesive did not reduce deformation in Usibor. The weld bonded beams (rubber weld bonded or epoxy weld bonded) had higher deformation and flange separation than the just resistance spot welded beams in the experimental tests.

The rubber-based adhesive did not reduce deformation of the Usibor beams and it was not powerful enough to keep the flanges together. Rubber-based adhesive failed cohesively. The tests showed that a stronger adhesive did not improve the results. Epoxy-based adhesive (type 2) was stronger than rubber based adhesive, but the epoxy-based adhesive failed by surface delamination (the Al-Si surface coating delaminated from the steel surface). The epoxy-based adhesive was strong, but it should not be used together with Usibor which has an Al-Si coating.

7. Future work and recommendations

It would be of interest to investigate rubber-based adhesive in different modes of loading than the 4-point bending, for instance axial crush testing for DP600 beams.

The adhesive model for simulating the rubber-based adhesive, did not give the same results as the experimental test. Further investigation of the rubber adhesive is necessary.

The rubber-based adhesive failed cohesively, but it still had some effect in deformation reduction, especially for the DP600 beams. Rubber-based adhesives could be used in applications where deformation reduction is desirable rather than preventing separation.

There was not benefit of using epoxy-based adhesive in combination with Usibor. The Al-Si surface coating was delaminated by the adhesive. It would be interesting to evaluate the contribution of adhesive with alternative coating for boron steel (which not requires full diffusion that causes brittle coating behavior). Testing boron steel without any coating could also be of interest.

In order to get accurate statistical values from the tests, the Usibor beams should be tested in more than three repetitions. It is recommended to run more tests for Usibor due to the divergent results.

References

- [1] Andreas Lutz, Detlef Symiet, 'Structural bonding of lightweight cars', Adhesion magazine, Dow automotive systems, 'n. d.' [online] Available from www.dow.com/scripts/litorder.asp?filepath=automotive/pdfs/noreg/299-51639.pdf&pdf=true [11 February 2011]

- [2] Dassault Systemes Simulia Corp. 'Prediction of B-Pillar Failure in Automobile Bodies' [published 1 March 2009], [online] Available from <http://www.techbriefs.com/component/content/article/5007> [20 January 2011]

- [3] ArcelorMittal Company 'Steels for hot stamping' [online] Available from <http://www.arcelormittal.com> [26 August 2010]

- [4] P. Nyström, M. Fermér, H. Nilsson, "The New Volvo V70 & XC70 Car Body", Euro Car Body, Bad Nauheim, Germany [October 2007]

- [5] F. Moroni , A. Pironi , F. Kleiner (July 2010), 'Experimental analysis and comparison of the strength of simple and hybrid structural joints'. International Journal of Adhesion and Adhesives, Elsevier, Volume 30, Issue 5, Pages 367-379

- [6] [Interview] Camilla Wästlund, Göteborg, Volvo Cars Corporation, March 2011

- [7] William Andrew Pub. (2008.07.30), Adhesives technology handbook, ISBN 0-8155-1533-2

- [8] A. Al-Samhan, A.M.H. Darwish (6 October 2002)' 'Strength prediction of weld-bonded joints', International Journal of Adhesion and Adhesives, Volume 23, Issue 1, Pages 23-28

- [9] William Andrew Pub. (2008.07.30), 'Adhesives technology handbook', ISBN 0-8155-1533- chapter 7, 11

- [10] Thomas Carlberger (2008), 'Adhesive joining for crashworthiness'. PhD thesis, Chalmers University, Gothenburg, Sweden, 2008

- [11] Mayo Clinic (2010), 'Occupational asthma' [online] Available from <<http://www.mayoclinic.com/health/occupational-asthma/DS00591/DSECTION=risk-factors>> [6 February 2011]
- [12] Rotech tooling Sweden (2009), 'Spot welding parameters' [Online] Available from <http://www.robot-welding.com/Welding_parameters.htm> [11 March 2011]
- [13] [Interview] Joel Lundgren, Göteborg, Volvo Cars Corporation, February 2011
- [14] Wieländer and Schill UK Ltd 'Boron steel' [online] Available from <<http://www.wielanderschill.co.uk/html/boronsteel.htm>> [19 February 2011]
- [15] T.B. Hilditch, J.G. Speer b, D.K. Matlock b. (25 October 2006), 'Effect of susceptibility to interfacial fracture on fatigue properties of spot-welded high strength sheet steel'. Elsevier, Volume 28, Issue 10, Pages 2566-2576
- [16] Rathbun RW, Matlock DK, Speer JG (August 2003). 'Fatigue behavior of spot welded high-strength sheet steel'. Welding Journal, Volume 82, no. 8, pp. 207-218.
- [17] Volvo Car Corporation Standard, VCS 5621, 19, Department 6857 Issued by Kristina Willstrand, issue 9, established 2010-08
- [18] N. Farabia, D.L. Chena, J. Lib, Y. Zhou and S.J. Dongc, [February 2010], 'Microstructure and mechanical properties of laser welded DP600 steel joints', Science direct, Volume 527, Issues 4-5, Pages 1215-1222
- [19] World auto steel, 'dual phase', [Online] Available from <<http://www.worldautosteel.org/SteelBasics/Steel-Types/Dual-Phase.aspx>>, 'n. d.' [9 April 2011]
- [20] Michael Ashby, David R. H. Jones (1992) [1986]. Engineering Materials 2, Oxford Press, ISBN 0-08-032532-7.
- [21] ArcelorMittal, Dual Phase steels, [Online] Available from <http://www.arcelormittal.com/automotive/products/europe/sheets/catalogue.pl?id_sheet=A1&header=&language=EN>, 'n. d.' [12 February 2011]

- [22] ASM Handbook Volume 1 'Properties and Selection', Irons, Steels, and High-Performance Alloys, Carbon and Low-Alloy Steels, Dual-Phase Steels
- [23] Flejes Industriales, Dual phase steel chemical composition, [online] Available from <<http://www.flinsa.com/documentos>> [25 March 2011]
- [24] Jennarong Tungtrongpaioj, Vitoon Uthaisangasuk and Wolfgang Bleck (2009), 'Determination of Yield Behaviour of Boron Alloy Steel at High Temperature'. Journal of Metals, Materials and Minerals. Vol. 19 No 1pp.29-39
- [25] M. Fermér, J. Jergeus, R. Johansson, J. K. Larsson, "Hot-Formed Steel in Car Body Structures", International Automotive Body Congress (IABC), Munich, Germany, September 22-23, 2010
- [26] Taylan Altan (December 2006), 'Hot-stamping boron-alloyed steels for automotive parts'. Stamping Journal [Online] Available from <<http://nsmwww.eng.ohio-state.edu/Dec06RDUpdate.pdf>>, [29 January 2011]
- [27] [Interview] Richard Johansson, Göteborg, Volvo Cars Corporation, March 2011
- [28] Corus, Boron Steels (2008) 'Boron Steels' [online] Available from <http://www.tatasteeleurope.com/file_source/Business%20Units/CORUS%20NARROW%20STRIP/BORON_STEEL_DS_2008.pdf.pdf> [January 2011]
- [29] Taylan Altan (December 2006), 'Hot-stamping boron-alloyed steels for automotive parts'. Stamping Journal [Online] Available from <<http://nsmwww.eng.ohio-state.edu/Dec06RDUpdate.pdf>>, [January 2011]
- [30] Masayoshi Suehiro, Jun Maki, Kazuhisa Kusumi, Masahiro Ohghami, Toshihiro Miyakoshi, (2003) 'Properties of Aluminum-coated Steels for Hot-forming', Nippon steel technical report No. 88
- [31] ArcelorMittal (2010) Steels for hot stamping, Very high strength steels [online] Available from <http://www.arcelormittal.com/automotive/products/europe/sheets/catalogue.pl?id_sheet=E&header=&language=EN> [5 January 2011]

Appendix 1. Classification of High Strength Steel

Steel	Yield strength (minimum) [MPa]
Mild steel (MS)	180
High strength steel (HSS)	180-280
Very high strength steel (VHSS)	280-380
Extra high strength steel (EHSS)	380-800
Ultra high strength steel (UHSS)	800

Appendix 2. Masses in CAE

The following masses were required to get the high and low deformations in CAE. The velocity was 10 m/s for all the beams.

	Mass [kg]	Spot weld spacing [mm]	Sheet thickness [mm]	
DP600				
	16 kg (H)	40mm/80mm	1,0	mm
	12 kg (L)	40mm/80mm	1,0	mm
	29 kg (H)	40mm/80mm	1,5	mm
	21 kg (L)	40mm/80mm	1,5	mm
Usibor				
	27 kg (H)	40mm/80mm	1,0	mm
	20 kg (L)	40mm/80mm	1,0	mm
	54 kg (H)	40mm/80mm	1,5	mm
	39 kg (L)	40mm/80mm	1,5	mm

(H) and (L) means high deformation and low deformation respectively.

Appendix 3. The planned test matrix

version	steel	thickness [mm]	joining method	spacing [mm]	quantity
1	DP	1,0	Rubber	40	6
2	DP	1,0	Rubber	80	4
3	DP	1,5	Rubber	40	4
4	DP	1,5	Rubber	80	4
5	DP	1,5	Epoxy	40	4
6	DP	1,0	Rsw	40	6
7	DP	1,0	Rsw	80	4
8	DP	1,5	Rsw	40	4
9	DP	1,5	Rsw	80	4
10	Boron	1,0	Rubber	40	6
11	Boron	1,0	Epoxy	40	6
12	Boron	1,5	Epoxy	40	6
13	Boron	1,0	Rsw	40	6
14	Boron	1,5	Rsw	40	6

Total number of tests: 70

Appendix 4.

version	steel	thickness [mm]	joining method	spacing [mm]	deformation	energy [J]	preference CAE			drop tower test	
							mass [kg]	velocity [m/s]	deformation [mm]	repetition	mass [mm]
1	DP	1,0	rsw	40	H	800	16	10	69	3	16
2	DP	1,0	rubber	40	H	800	16	10	60	3	16
3	DP	1,0	rsw	40	L	600	12	10	46	3	16
4	DP	1,0	rubber	40	L	600	12	10	40	3	16
5	DP	1,0	rsw	80	H	800	16	10	72	2	16
6	DP	1,0	rubber	80	H	800	16	10	61	2	16
7	DP	1,0	rsw	80	L	600	12	10	51	2	16
8	DP	1,0	rubber	80	L	600	12	10	40	2	16
9	DP	1,5	rsw	40	H	1450	29	10	66	2	32
10	DP	1,5	rubber	40	H	1450	29	10	62	2	32
11	DP	1,5	epoxy	40	H	1450	29	10	62	2	32
12	DP	1,5	rsw	40	L	1050	21	10	44	2	16
13	DP	1,5	rubber	40	L	1050	21	10	41	2	16
14	DP	1,5	epoxy	40	L	1050	21	10	41	2	16
15	DP	1,5	rsw	80	H	1450	29	10	72	2	32
16	DP	1,5	rubber	80	H	1450	29	10	63	2	32
17	DP	1,5	rsw	80	L	1050	21	10	48	2	16
18	DP	1,5	rubber	80	L	1050	21	10	41	3	16
19	Boron	1,0	rsw	40	H	1350	27	10	66	3	32
20	Boron	1,0	rubber	40	H	1350	27	10	60	3	32
21	Boron	1,0	epoxy	40	H	1350	27	10	60	3	32
22	Boron	1,0	rsw	40	L	1000	20	10	44	3	16
23	Boron	1,0	rubber	40	L	1000	20	10	41	3	16
24	Boron	1,0	epoxy	40	L	1000	20	10	41	3	16
25	Boron	1,5	rsw	40	H	2700	54	10	67	3	32
26	Boron	1,5	epoxy	40	H	2700	54	10	64	3	32
27	Boron	1,5	rsw	40	L	1350	27	10	45	3	32
28	Boron	1,5	epoxy	40	L	1350	27	10	41	3	32

Appendix 5. Full test matrix

This matrix was performed as experimental 4-point bending test

Number	Version	Beam identity	Steel	Thickness [mm]	Joining method [mm]	Spacing [mm]	Deformation [high or low]	Mass [kg]	Height [m]	Desired velocity [m/s]	Velocity obtained in test [m/s]	Max dynamic deformation [mm]	Max static deformation [mm]	Test number according to photos (also test order)	Spring back [mm]	Comment
1	1	D1N4010	DP	1,0	rsw	40	H	16	5,1	10,0	10,1	115	75	7	40	
2		D2N4010	DP	1,0	rsw	40	H	16	5,1	10,0	10,1	115	75	8	40	
3		D3N4010	DP	1,0	rsw	40	H	16	5,1	10,0	10,1	114	75	9	39	
4	2	D1R4010	DP	1,0	rubber	40	H	16	5,1	10,0	10,1	90	59	10	31	
5		D2R4010	DP	1,0	rubber	40	H	16	5,1	10,0	10,1	90	59	11	31	
6		D3R4010	DP	1,0	rubber	40	H	16	5,1	10,0	10,1	92	59	12	33	
7	3	D1N4010	DP	1,0	rsw	40	L	16	3,8	8,7	8,7	87	52	17	35	
8		D2N4010	DP	1,0	rsw	40	L	16	3,8	8,7	8,7	84	49	18	35	
9		D3N4010	DP	1,0	rsw	40	L	16	3,8	8,7	8,7	85	52	19	33	
10	4	D1R4010	DP	1,0	rubber	40	L	16	3,8	8,7	8,7	70	37	20	33	
11		D2R4010	DP	1,0	rubber	40	L	16	3,8	8,7	8,7	70	40	21	30	
12		D3R4010	DP	1,0	rubber	40	L	16	3,8	8,7	8,7	70	37	22	33	
13	5	D1N8010	DP	1,0	rsw	80	H	16	5,1	10,0	10,1	114	76	3	38	
14		D2N8010	DP	1,0	rsw	80	H	16	5,1	10,0	10,1	110	75	4	35	
15	6	D1R8010	DP	1,0	rubber	80	H	16	5,1	10,0	10,1	110	77	5	33	
16		D2R8010	DP	1,0	rubber	80	H	16	5,1	10,0	10,1	115	75	6	40	
17	7	D1N8010	DP	1,0	rsw	80	L	16	3,8	8,7	8,7	90	58	13	32	
18		D2N8010	DP	1,0	rsw	80	L	16	3,8	8,7	8,6	85	58	14	27	
19	8	D1R8010	DP	1,0	rubber	80	L	16	3,8	8,7	8,7	75	42	15	33	
20		D2R8010	DP	1,0	rubber	80	L	16	3,8	8,7	8,7	75	40	16	35	

Appendix 5. Full test matrix

Number	Version	Beam identity	Steel	Thickness [mm]	Joining method [mm]	Spacing [mm]	Deformation [high or low]	Mass [kg]	Height [m]	Desired velocity [m/s]	Velocity obtained in test [m/s]	Max dynamic deformation [mm]	Max static deformation [mm]	Test number according to photos (also test order)	Spring back [mm]	Comment
21	9	D1N4015	DP	1,5	rsw	40	H	32	4,6	9,5	9,5	-	67	44	-	no dynamic disp
22		D2N4015	DP	1,5	rsw	40	H	32	4,6	9,5	9,5	-	75	45	-	no dynamic disp
23	10	D1R4015	DP	1,5	rubber	40	H	32	4,6	9,5	9,3	90	65	46	25	<i>wrong velocity</i>
24		D2R4015	DP	1,5	rubber	40	H	32	4,6	9,5	9,5	93	68	47	25	
25	11	D1E4015	DP	1,5	epoxy	40	H	32	4,6	9,5	9,5	86	57	48	29	
26		D2E4015	DP	1,5	epoxy	40	H	32	4,6	9,5	9,5	87	64	49	23	
27	12	D1N4015	DP	1,5	rsw	40	L	16	6,7	11,5	11,5	80	49	71	31	
28		D1N4015	DP	1,5	rsw	40	L	16	6,7	11,5	11,5	80	49	72	31	
29	13	D1R4015	DP	1,5	rubber	40	L	16	6,7	11,5	11,5	72	47	73	25	
30		D2R4015	DP	1,5	rubber	40	L	16	6,7	11,5	11,4	71	39	74	32	
31	14	D1E4015	DP	1,5	epoxy	40	L	16	6,7	11,5	11,5	70	42	75	28	
32		D2E4015	DP	1,5	epoxy	40	L	16	6,7	11,5	11,5	72	42	76	30	
33	15	D1N8015	DP	1,5	rsw	80	H	32	4,6	9,5	9,5	110	73	52	37	
34		D2N8015	DP	1,5	rsw	80	H	32	4,6	9,5	9,5	111	77	51	34	
35	18	D1R8015	DP	1,5	rubber	80	H	32	4,6	9,5	9,5	95	67	53	28	
36		D2R8015	DP	1,5	rubber	80	H	32	4,6	9,5	9,5	90	55	54	35	
37	17	D1N8015	DP	1,5	rsw	80	L	16	6,7	11,5	11,5	85	52	77	33	
38		D2N8015	DP	1,5	rsw	80	L	16	6,7	11,5	11,4	84	56	78	28	
39	18	D1R8015	DP	1,5	rubber	80	L	16	6,7	11,5	11,4	75	43	79	32	
40		D2R8015	DP	1,5	rubber	80	L	16	6,7	11,5	11,4	74	46	80	28	

Appendix 5. Full test matrix

Number	Version	Beam identity	Steel	Thickness [mm]	Joining method [mm]	Spacing [mm]	Deformation [high or low]	Mass [kg]	Height [m]	Desired velocity [m/s]	Velocity obtained in test [m/s]	Max dynamic deformation [mm]	Max static deformation [mm]	Test number according to photos (also test order)	Spring back [mm]	Comment
41	19	B1N4010	Boron	1,0	Rsw	40	H	32	4,3	9,2	9,2	93	52	36	41	
42		B2N4010	Boron	1,0	Rsw	40	H	32	4,3	9,2	-	-	-	-	-	no velocity
43		B3N4010	Boron	1,0	Rsw	40	H	32	4,3	9,2	-	-	-	-	-	no velocity
44	20	B1R4010	Boron	1,0	Rubber	40	H	32	4,3	9,2	9,2	97	51	37	46	
45		B2R4010	Boron	1,0	Rubber	40	H	32	4,3	9,2	9,2	97	51	38	46	
46		B3R4010	Boron	1,0	Rubber	40	H	32	4,3	9,2	9,2	115	68	39	47	
47	21	B1E4010	Boron	1,0	Epoxy	40	H	32	4,3	9,2	9,2	100	55	40	45	
48		B2E4010	Boron	1,0	Epoxy	40	H	32	4,3	9,2	9,2	93	43	41	50	
49		B3E4010	Boron	1,0	Epoxy	40	H	32	4,3	9,2	9,2	93	70	42	23	
50	22	B1N4010	Boron	1,0	Rsw	40	L	16	6,4	11,2	11,3	80	32	25	48	
51		B2N4010	Boron	1,0	Rsw	40	L	16	6,4	11,2	11,2	80	32	26	48	
52		B3N4010	Boron	1,0	Rsw	40	L	16	6,4	11,2	11,2	80	33	27	47	
53	23	B1R4010	Boron	1,0	Rubber	40	L	16	6,4	11,2	11,3	75	32	28	43	
54		B2R4010	Boron	1,0	Rubber	40	L	16	6,4	11,2	11,3	80	32	29	48	
55		B3R4010	Boron	1,0	Rubber	40	L	16	6,4	11,2	11,3	80	27	30	53	
56	24	B1E4010	Boron	1,0	Epoxy	40	L	16	6,4	11,2	11,3	75	32	31	43	
57		B2E4010	Boron	1,0	Epoxy	40	L	16	6,4	11,2	11,2	75	27	32	48	
58		B3E4010	Boron	1,0	Epoxy	40	L	16	6,4	11,2	11,3	73	34	33	39	
59	25	B1N4015	Boron	1,5	Rsw	40	H	32	8,6	13,0	13,1	100	53	57	47	
60		B2N4015	Boron	1,5	Rsw	40	H	32	8,6	13,0	13,0	120	75	58	45	

Appendix 5. Full test matrix

Number	Version	Beam identity	Steel	Thickness [mm]	Joining method [mm]	Spacing [mm]	Deformation [high or low]	Mass [kg]	Height [m]	Desired velocity [m/s]	Velocity obtained in test [m/s]	Max dynamic deformation [mm]	Max static deformation [mm]	Test number according to photos (also test order)	Spring back [mm]	Comment
61		B3N4015	Boron	1,5	Rsw	40	H	32	8,6	13,0	-	-	-	-	-	no velocity
62	26	B1E4015	Boron	1,5	Epoxy	40	H	32	8,6	13,0	13,0	100	56	59	44	
63		B2E4015	Boron	1,5	Epoxy	40	H	32	8,6	13,0	-	93	49	60	44	<i>no velocity</i>
64		B3E4015	Boron	1,5	Epoxy	40	H	32	8,6	13,0	13,0	105	61	61	44	
65	27	B1N4015	Boron	1,5	Rsw	40	L	32	6,2	11,0	11,1	85	37	64	48	
66		B2N4015	Boron	1,5	Rsw	40	L	32	6,2	11,0	11,1	90	37	65	53	
67		B3N4015	Boron	1,5	Rsw	40	L	32	6,2	11,0	11,1	87	47	66	40	
68	28	B1E4015	Boron	1,5	Epoxy	40	L	32	6,2	11,0	11,1	70	37	67	33	
69		B2E4015	Boron	1,5	Epoxy	40	L	32	6,2	11,0	11,1	75	40	68	35	
70		B2E4015	Boron	1,5	Epoxy	40	L	32	6,2	11,0	11,1	75	39	69	36	

Appendix 5. Full test matrix

Table for extra beams (calibration)

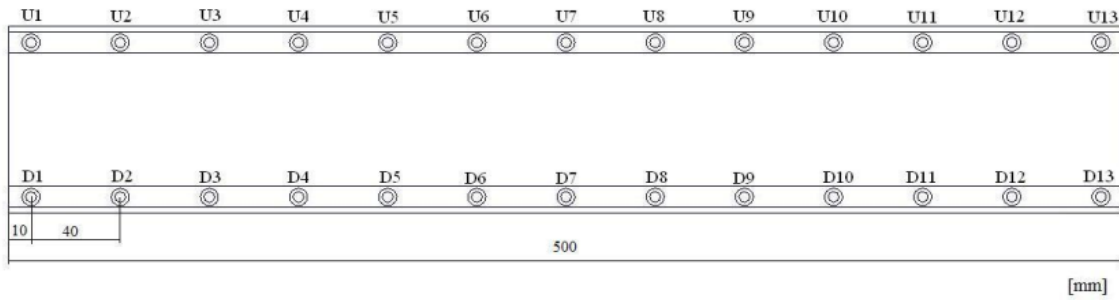
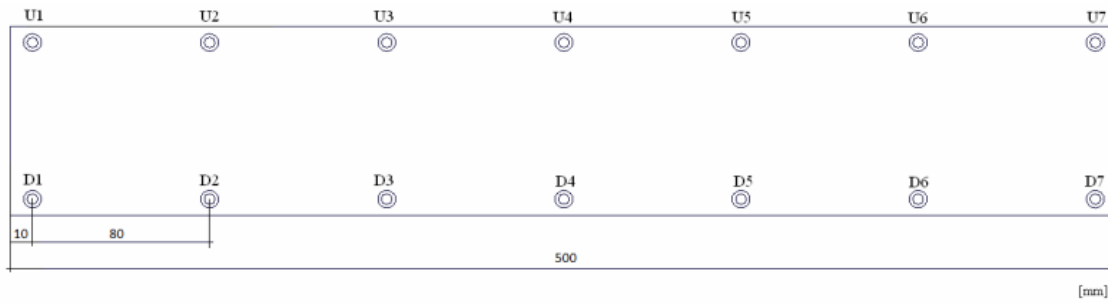
Number	Version	Beam identity	Steel	Thickness [mm]	Joining method [mm]	Spacing [mm]	Deformation [high or low]	Mass [kg]	Height [m]	Desired velocity [m/s]	Velocity obtained in test [m/s]	Max dynamic deformation [mm]	Max static deformation [mm]	Test number according to photos (also test order)	Spring back [mm]	Comment
71	1	D1N4010	DP	1,0	rsw	40	H	16	5,1	10	-	-	-	-	-	
72		D2N4010	DP	1,0	rsw	40	H	16	5,1	10	-	-	-	-	-	
73	3	D1N4010	DP	1,0	rsw	40	L	16	3,8	8,7	-	-	-	-	-	
74		D2N4010	DP	1,0	rsw	40	L	16	3,8	8,7	-	-	-	-	-	
75	5	D1N8010	DP	1,0	rsw	80	H	16	5,1	10	10,1	140	123	2	17	high static max def.
76		D2N8010	DP	1,0	rsw	80	H	16	5,1	10	7,9	90	-	1		wrong velocity
77	7	D1N8010	DP	1,0	rsw	80	L	16	3,8	8,7	-	-	-	-	-	
78		D2N8010	DP	1,0	rsw	80	L	16	3,8	8,7	-	-	-	-	-	
79	9	D1N4015	DP	1,5	rsw	40	H	32	4,6	9,5	9,5	-	73	43	30	
80	12	D1N4015	DP	1,5	rsw	40	L	16	6,7	11,5	11,3	75	52	70	23	wrong velocity
81	15	D1N8015	DP	1,5	rsw	80	H	32	4,6	9,5	9,5	-	77	50	-	
82	17	D1N8015	DP	1,5	rsw	80	L	16	6,7	11,5	11,4	90	50	81	40	

Appendix 5. Full test matrix

Table for extra beams (calibration)

Number	Version	Beam identity	Steel	Thickness [mm]	Joining method [mm]	Spacing [mm]	Deformation [high or low]	Mass [kg]	Height [m]	Desired velocity [m/s]	Velocity obtained in test [m/s]	Max dynamic deformation [mm]	Max static deformation [mm]	Test number according to photos (also test order)	Spring back [mm]	Comment
83	19	B1N4010	Boron	1,0	rsw	40	H	32	4,3	9,2	9,2	91	53	34	38	
84		B2N4010	Boron	1,0	rsw	40	H	32	4,3	9,2	9,2	92	49	35	43	
85	22	B3N4010	Boron	1,0	rsw	40	L	16	6,4	11,2	11,2	75	32	23	43	
86		B4N4010	Boron	1,0	rsw	40	L	16	6,4	11,2	11,2	80	32	24	48	
87	25	B1N4015	Boron	1,5	rsw	40	H	32	8,6	13,0	-	100	55	55	45	<i>no velocity</i>
88		B2N4015	Boron	1,5	rsw	40	H	32	8,6	13,0	13,0	105	62	56	43	
89	27	B3N4015	Boron	1,5	rsw	40	L	32	6,2	11,0	11,1	80	44	63	36	<i>wrong velocity</i>
90		B4N4015	Boron	1,5	rsw	40	L	32	6,2	11,0	11,2	84	43	62	41	<i>wrong velocity</i>

Appendix 6. Comments for each beam



The pictures enable identification of the defective spot welds and the position of the failed adhesive. Use this picture together with the following matrix in the next pages.

Appendix 6. Comments for each beam

See the previous page to identify the defective spot weld and failed adhesive position.

A = defective spot

C = separation of flange

U = position up

B = crack

D = adhesive separation

D = position down

test order	version	joining method	A	B	C.	D.	comment
1	DP	RSW					Scrap
2	80 mm				x		unsymmetric deformation
3	1.0 mm				x		C. U and D
4	H				x		C. U and D
5		rubber				x	D. U3, U5, D3, D5
6						x	D. U3, U5, D3, D5
7	DP	RSW					all good
8	40 mm						all good
9	1.0 mm						all good
10	H	rubber				x	D. starts to separate at U6, U9
11						x	D. starts to separate at U6, U9, D6, D9
12						x	D. starts to separate at U6, U9, D6, D9
13	DP	RSW			x		C. very small in U and D
14	80 mm				x		C. very small in U and D
15	1.0 mm	rubber				x	D. U5, U9, D5, D9
16	L					x	D. U5, U9, D5, D9
17	DP	RSW					all good
18	40 mm						all good
19	1.0 mm						all good
20	L	rubber				x	D. starts to separate U and D, satisfactory weld spot
21						x	D. starts to separate U and D, satisfactory weld spot
22						x	D. starts to separate U and D, satisfactory weld spot

Appendix 6. Comments for each beam

A = defective spot

C = seperation of flange

U = position up

B = crack

D = adhesive seperation

D = position down

test order	version	joining method	A	B	C.	D.	comment
23	Boron	RSW	X	x	x		A. U9 B. 2 crack in hat
24	40 mm		X	x	x		A. U9 B. 2 crack in hat
25	1.0 mm		X	x	x		A. U9 B. 2 crack in hat
26	L		X	x	x		A. U9 B. 2 crack in hat
27			X	x	x		A. U5, U9, U10, D5, D9, D10 B. 2 crack in hat
28		rubber	X			x	A. U5, U9, D4, D8
29			X			x	A. U5, U9, D5, D9
30				x		x	B. U9, D9
31		epoxy	X			x	A. U5, U9, D5, D9
32			X			x	A. U5, U9, D5, D9
33			X			x	A. U5, U9, D5, D9
34	Boron	RSW	X	x	x		A. U9, D5, D9 B. 4 cracks in hat C. big separate in D9
35	40 mm		X	x	x		A. U5, U9, D5, D9 B. 4 cracks in hat
36	1.0		X	x	x		A U5, U9, U10, D5, D10 B. 4 cracks C. U9, D9
37	H	rubber	X	x		x	A. U4, U5, U9, D4, D5, D9 B. 3 cracks D. D5, D9 big separate.
38			X	x		x	A. U4, U5, U9, D4, D5, D9 B. 3 cracks D. D5, D9 big separate.
39			X	x		x	A. U4, U5, U9, D4, D5, D9 B. 2 cracks at U D. big separate. at D4, D5 U4, U5
40		epoxy	X	x			A. U5, U9, D5, D9 B. 2 cracks at U
41			X	x			A. U5, U9, D5, D9 B. 3 cracks
42			X	x			A. U5,U9, D5, D9, D10 B. 2 cracks U
43*	DP	RSW			x		C. starts to separate.
44	40mm				x		C. starts to separate.
45	1,5 mm				x		C. starts to separate.
46	H	Rubber			x	x	C. starts to separate. D. starts to separate
47					x	x	C. starts to separate. D. starts to separate
48		epoxy					all good
49							all good

Appendix 6. Comments for each beam

A = defective spot

C = seperation of flange

U = position up

B = crack

D = adhesive seperation

D = position down

test order	version	joining method	A	B	C.	D.	comment
50	DP	RSW			x		satisfactory weld spot
51	80mm				x		satisfactory weld spot
52	1,5mm				x		satisfactory weld spot
53	H	rubber			x	x	C. separation as in test 50
54					x	x	C. separation as in test 50
55	Boron	RSW	X	x			No registration of velocity! A. U5,U9,U10, D4, D5, D9, D10 B. 2 cracks U
56	40mm		X	x			A. U5,U9,U10, D4, D5, D9, D10 B. 2 cracks U
57	1,5mm		X	x			A. U5,U9,U10, D4, D5, D9, D10 B. 2 cracks U
58	H		X				A. U2, U3, U4, U5, U9, D2, D3, D4, D5, D9 C. huge separation of hat-lid
59		epoxy	X	x			A. U4, U5, U9, D4, D5, D9 B. 1 crack at U5
60			X	x			No registration of velocity! A. U4, U5, U9, D4, D5, D9 B. 1 crack at U5
61			X			x	A. U2, U3, U4, U5, U9, D2, D3, D4, D5, D9 C. huge separation of hat-lid
62	Boron	RSW	X	x			A. U5,U9,U10, D5, D9, D10 B. 1 crack at U5
63	40mm		X				A. U5,U9,U10, D5, D9, D10
64	1,5mm		X				A. U5, U9, D5, D9
65	L		X	x			A. U3, U4, U5, U9, U10, D3, D4, D5, D9, D10, D11 B. 1 crack
66			X				A. U5, U7, U8, U9, D3, D4, D5, D9, D10, D11, D12 B. 1 crack
67		epoxy	X			x	A. U5, U9, U10, D5
68			X			x	A. U4, U5, U9, D4, D5, D9
69			X			x	A. U5, U9, U10, D5, D9, D10

Appendix 6. Comments for each beam

A = defective spot

C = seperation of flange

U = position up

B = crack

D = adhesive seperation

D = position down

test order	version	joining method	A	B	C.	D.	comment
70	DP	RSW					satisfactory weld spot, small separation in impact area- no failure
71	40mm						satisfactory weld spot small separation in impact area- no failure
72	1,5mm				x		starts to separate in impact area
73	L	rubber				x	adhesive starts to separate in impact area
74							no separation at all
75		epoxy					no separation at all
76							no separation at all
77	DP	RSW			x		satisfactory weld spot
78	80mm				x		satisfactory weld spot
79	1,5mm	rubber			x	x	satisfactory weld spot C. buckle less than test nr 77
80	L				x	x	satisfactory weld spot
81		RSW			x		satisfactory weld spot

Appendix 7. The adhesive do not reduce the separation of the flanges of Usibor beams



VOLVO
: POSTry
Name of Test Object : vehicle #1
Customer Test No. : 11609381
Test No. : 11609381

Figure 1. 40 mm spot weld spacing at low deformation. From top RSW, rubber, epoxy



VOLVO
: POSTry
Name of Test Object : vehicle #1
Customer Test No. : 11609381
Test No. : 11609381

Figure 2. 40 mm spot weld spacing at high deformation. From top RSW, rubber, epoxy



VOLVO
: POSTry
Name of Test Object : vehicle #1
Customer Test No. : 11609381
Test No. : 11609381

Figure 3. 40 mm spot spacing at low deformation. From top RSW, epoxy

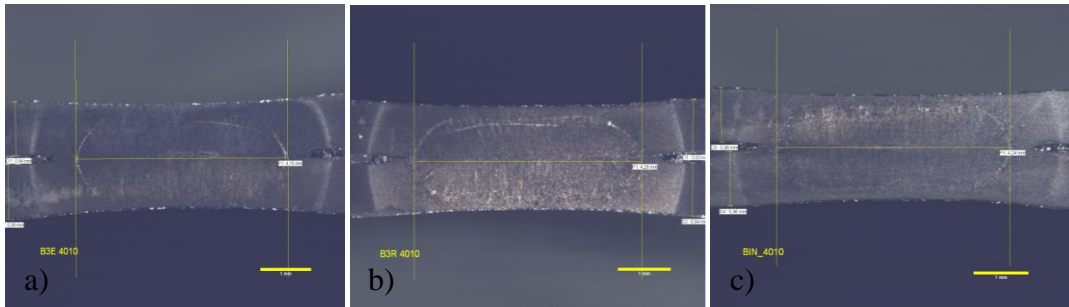


VOLVO
: POSTry
Name of Test Object : vehicle #1
Customer Test No. : 11609381
Test No. : 11609381

Figure 4. 40 mm spot weld spacing at high deformation. From top RSW, epoxy

Figure 1, 2, 3 and 4 shows the separation of boron beams. The weld bonded beams had larger separation than the resistance spot welded beams.

Appendix 8. Microscopic cross section of the nugget



a) Cross section cut of the epoxy weld bonded beam of sheet thickness 1,0 mm. The measured nugget size is 4,16 mm in diameter.

b) Cross section cut of a rubber weld bonded beam of sheet thickness 1,0 mm. The measured nugget size is 2,24 mm in diameter.

c) Cross section cut of a resistance spot welded beam of sheet thickness 1,0 mm. The measured nugget size is 2,24 mm in diameter.